

## Influencing parameter optimisation of CRDI engine fuelled with lemongrass biodiesel blends

Paramasivam Prakash & Chinnathambi Dhanasekaran

To cite this article: Paramasivam Prakash & Chinnathambi Dhanasekaran (2022): Influencing parameter optimisation of CRDI engine fuelled with lemongrass biodiesel blends, International Journal of Ambient Energy, DOI: [10.1080/01430750.2022.2142286](https://doi.org/10.1080/01430750.2022.2142286)

To link to this article: <https://doi.org/10.1080/01430750.2022.2142286>



Published online: 21 Nov 2022.



Submit your article to this journal [↗](#)



View related articles [↗](#)



View Crossmark data [↗](#)



# Influencing parameter optimisation of CRDI engine fuelled with lemongrass biodiesel blends

Paramasivam Prakash  and Chinnathambi Dhanasekaran

Department of Mechanical Engineering, VELS Institute of Science, Technology & Advanced Studies (VISTAS), Chennai, India

## ABSTRACT

Based on the central composite design of the experiment of 50 input combinations, the behaviour of common rail direct injection compressed ignition engine was examined, and maximum engine performance and minimal emission were found using multi-objective RSM. The optimal input combination was identified after thorough testing. It consisted of 12.3 kg engine load, 60% lemongrass biodiesel, 1000 bar FIP, 6°bTDC FIT, and 0% exhaust gas recirculation. A second order quadratic model with  $R^2$  values of 0.99, 0.99, 0.84, 0.98, 0.82, 0.93 and 0.94 for Torque, BMEP, BTE, mechanical efficiency, BSFC, CO and NO<sub>x</sub>, respectively, was developed by taking into account all of the input parameters for all of the investigated responses. This model can be used to predict output responses within the experimental analysis ranges, with a maximum combined desirability of 0.863. ANN model may be successfully implemented for better prediction of the engine each output response than RSM-based prediction.

## Highlights

- CCD-based DOE was made in the design expert 13 version by considering major influencing CRDI engine parameters. RSM was used to create a second-order polynomial quadratic model for forecasting torque, BMEP, mechanical efficiency, BTE, BSFC, CO and NO<sub>x</sub>. Furthermore, there was no apparent difference between the fitted values and the experimental data.
- The optimisation was done to enhance the BMEP, Torque, BTHE, and mechanical efficiency and minimise the BSFC, CO and NO<sub>x</sub>.
- The optimum combination for the best performance is obtained when running the engine at the following settings such as 100% EL, 60% fuel blend, 6°bTDC of FIT, 1000 bar FIP and 0% EGR.
- The ANOVA study's findings indicate that EL has a 99% impact on BMEP and torque. The effect of EL on BTHE is 60.3%. EL affects 94.4% of mechanical efficiency. EL controls 55.9% of SFC. CO is influenced by EL, EGR and IT, respectively, by 60.58%, 10% and 5.3%. EGR and IT both affect NO<sub>x</sub> by 50.5% and 23.9%, respectively.
- CRDI engine output response prediction accuracy of ANN is better than RSM

## ARTICLE HISTORY

Received 8 April 2022  
Accepted 17 October 2022

## KEYWORDS

Lemongrass biodiesel; CRDI engine; RSM; performance and emission characteristics; optimisation; ANN

## Nomenclature

FB	fuel blend
FIP	fuel injection pressure
EGR	exhausts gas recirculation
CCD	central composite design
CRDI	common rail direct injection diesel engine
BMEP	brake mean effective pressure
CO	carbon monoxide
HC	hydro carbon
NO <sub>x</sub>	oxides of Nitrogen
BP	brake power
ppm	parts per million
LGO	lemon grass oil
bTDC	before top dead centre
PM	particulate matter
S/N ratio	signal to noise

FB60%	(60% of Lemongrass Biodiesel + 40% of Diesel)
FB30%	(30% of Lemongrass Biodiesel + 70% of Diesel)
B100	100% of biodiesel
ECU	electronic control unit

## Symbols

N.m	Newton metre
°C	degree Celsius
mm	millimetre
cm	centimetre
@	at
CC	cubic centimetre
Kg	kilogram
Kw	kilowatt
%	percentage

EL	engine load
FIT	fuel injection timing
RSM	response surface methodology
BBD	Box behnken design
BTE	brake thermal efficiency
BSFC	brake specific fuel consumption
EGT	exhaust gas temperature
LOME	linseed oil methyl ester
CO <sub>2</sub>	carbon dioxide
DOE	design of experiment
CR	compression ratio
LGO25	lemongrass oil 25%+75% diesel
ANOVA	analysis of variance
KOH	potassium hydroxide
ASTM	American standard test method
FB45%	(45% of Lemongrass Biodiesel + 55% of Diesel)
FB15%	(15% of Lemongrass Biodiesel + 85% of Diesel)
Cao	calcium oxide

## 1. Introduction

Fuels are used for various applications, including power generation, automotive transportation, industrial processes, and residential use. As the population transitions to a more affluent lifestyle and technology progresses, fuel consumption increases hour by hour. As a result, fuel plays a significant role in all facets of human life. Currently, India imports petroleum from foreign countries to meet its energy demands. Almost three by fourth of India's energy demand is met by refining imported crude oil. Hence a significant portion of our GDP (gross domestic product) is spent on crude oil imports from other nations.

According to data, we spent INR 427.45 billion on petroleum imports in September 2020, compared to INR 614.68 billion in 2014. India's GDP was predicted to be Rs 26.9 trillion in the first quarter of fiscal year 20-21. We have spent an average of Rs 427.45 billion per financial year from this fund. It is obvious from this data that the government's expenditure on gasoline imports has decreased dramatically as a result of the COVID19 pandemic crisis. Countries all around the world have seen economic slowdowns, and oil-exporting countries, particularly those in the Gulf, have seen a drop in demand for petroleum products. The price of crude oil per barrel has fallen as a result of these factors. However, once negative economic conditions such as COVID19 and the global economic crisis have passed, the price of crude oil may climb, forcing developing countries such as India to spend large sums on petroleum products, perhaps returning to former highs. To overcome their excessive reliance on petroleum exporting countries for crude oil imports, petroleum-importing countries must focus more on alternative sources such as solar, wind, gas and biofuels, which are environmentally beneficial and referred to as green energy. In a life cycle analysis, these sources produce a lower percentage of carbon monoxide, hydrocarbons and carbon dioxide.

We can protect the environment by using these green energies, particularly biodiesel. As a result, countries all over the world must create policies to promote biodiesel research and development. The following reasons explain why countries around the world should focus more on green energies like biodiesel: conventional energy generation has resulted in

increased carbon emissions; nonrenewable energy sources such as coal, nuclear energy and fossil fuels contribute to environmental degradation by emitting more carbon. The use of this energy has a negative influence not just on the environment but also on humans, animals and species' livelihoods. Because of our overdependence on conventional energy, particularly petroleum products, the entire globe has been exploring viable strategies to avoid ozone layer depletion, acid rain and climate change. Other advantages of biofuel include its environmental friendliness, lack of sulfur and particle content, and the fact that it may be generated at any time with a lower fuel preparation plant installation cost.

As a result of the growing population, the demand for petroleum oil is increasing, resulting in increased air pollution, prompting the search for cleaner fuel. Due to the alarming situation of energy driving the scientist to find locally available, environment friendly and must be renewable sources of fuel, the nature of the feedstock. Performance and emissions depend on the usage of different types of engines, biodiesel chemical composition, type of diesel fuel and measurement techniques. Hence it is difficult to establish the relationship between these; moreover, density depends on the chain length of the esters, presence of high saturated esters leads to increased cetane number, lower iodine number and density than unsaturated esters, but high unsaturated esters lead to better viscosity, cold flow properties and poor oxidation stability (N. Kumar, Varun, and Chauhan 2013). Lemongrasses are mostly available in south India, particularly Cochin, Karnataka and Tamilnadu, due to the production and exportation of lemongrass, also called Cochin grass. Lemongrass oil contains rich bioactive compounds and is generally used in cosmetic, pharmaceutical and food preservation applications (Mukarram et al. 2022). Essential oils of *Cymbopogon nardus* are valuable alternatives in handling pest insects in the stored room and acting as a repellent (Caballero-Gallardo et al. 2021). To improve performance and exhaust, diesel fuel is blended with biodiesel fuel. And also, CI engine performance depends on various combinations of influencing parameters like the quantity of fuel injected, timing of fuel injection in the combustion chamber, fuel injection pressure, dimension of the combustion chamber, dimension of nozzles and pattern of fuel spray etc., (Ganesan, Senthil Kumar, and Hemanandh 2020). Investigated by changing the kapok methyl ester blend (at B20, B30, B40) and by changing injector hole number (at 4, 5, 6), revealed that maximum brake thermal efficiency were achieved at higher fuel blend and higher fuel injector hole and also HC, CO, NO<sub>x</sub>, smoke and brake specific fuel consumption decreased significantly by increasing the number of injector hole (Narayanan, Ramesh, and Sakthivel 2019). Better fuel burning in the cylinder was reported using seven hole nozzle (S, K, and R 2019). Lemon grass biodiesel plus mint biodiesel called dual fuel blended with diesel at different proportions and concluded based on experimental engine run as thermal brake efficiency and NO<sub>x</sub> increases, but the CO, HC, CO<sub>2</sub>, fuel consumption decreases with an increase of fuel blend (Senthil Kumar and Ramesh Babu 2020). Investigated the LGO blended with diesel in direct injection single cylinder agricultural diesel engine, fuel prepared at B25, B50, B75, B100 and diesel as a reference fuel. Concluded that LGO can be used as a fuel by directly mixing with diesel in a diesel engine without any modifications and also observed the NO<sub>x</sub>, heat

release rate and cylinder pressure increase. Still, calorific value, iodine index, BTE, CO, HC and smoke emissions were lower than diesel in all four test fuel combinations (Sathiyamoorthi et al. 2021b). Methyl ester of Palmarosa bio material blends with conventional diesel investigated in a single cylinder diesel engine by varying injection pressure of 200, 225, 250 bars in a combustion chamber with a fixed volume and observed longer and shorter spray tip penetrations. Revealed that spray cone angle of 17.5 and 11.4 ms for Palmarosa biodiesel and diesel. The fuel spray's main influencing parameters are the fuel's density and viscosity. Increasing injection pressure leads to faster combustion with a shorter duration than lower injection pressure (Sathiyamoorthi et al. 2021a). Fuel spray penetration length depends on nozzle hole diameter and injection pressure, and penetration length was increased with high FIP and larger hole diameter (Algayyim, Wandel, and Yusaf 2018; Ge et al. 2020). Investigated CRDI engine by varying engine load, biodiesel blend concentration and EGR and revealed that these engine parameters and fuel properties have a greater influence on PM emissions and the PM emissions are reduced at 30% palm biodiesel blend and 10% of EGR. The performance of the test fuel was further improved by adding a nano-sized emulsion additive (Elkelawy et al. 2020). The performance of blended algae biodiesel was further improved by adding 15 ml of n-pentane per litre of blended fuel (Elkelawy et al. 2021). Cao heterogeneous catalyst-based transesterification was carried out for the production of biodiesel. concluded the optimum performance and emission parameters as 2.258 kW of BP, 29.05% of BTE, 6.31 PPM of HC, 159.5 PPM of NO<sub>x</sub> at 8.05 kg of load, CR of 18, 180 bar FIP based on the desirability approach using RSM (Singh et al. 2020). 93.2% of biodiesel from *Pithecellobium dulce* seed oil was achieved at 1:6, 60°C, 0.8 wt%, 90 min of molar ratio, reaction temperature, catalyst, reaction time and reported that CO, HC and NO<sub>x</sub> decreased but the CO<sub>2</sub> and smoke intensity increased (Chandra Sekhar et al. 2018). 93.38% biodiesel yield from the mixture of sunflower and soybean oil following BBD-based RSM, and reported the optimum point is 203.5 ml of methanol per litre of oil, 0.57 wt% homogeneous catalyst, 52 min reaction time and 530 rpm of speed. CCD-based performance and emission optimisation of EL of 2.05 kW and 70% blend ratio recommended that sunflower/soybean oil biodiesel blended upto 70% with diesel (Elkelawy et al. 2020). Sunflower and soybean oil mixture-based biodiesel production optimisation and analysed of diesel engine performance and emissions by blending 30, 50 and 70% with diesel fuel (Elkelawy et al. 2019). Cotton seed biodiesel produced by the transesterification process and the blends of biodiesel behaviour by adding bioethanol were investigated. And reported the oxygenated blend effect as higher SFC, BTE and CO emissions are lower, and HC emissions slightly increased. The oxygenated fuel blends gave a promising alternative for diesel fuel irrespective of CO<sub>2</sub> and HC emissions (Elkelawy et al. 2018). CO, HC and NO<sub>x</sub> emissions are decreased by adding an additive of nanothiocyanate due to surface/volume ratio and micro explosion phenomena (Elkelawy et al. 2021). Liquid or solid-based additives improve combustion and emission problems such as poor combustion and an increase in NO<sub>x</sub> and HC. Reported that CO, HC and, smoke density, NO<sub>x</sub> decreased by increasing the dose of Cyclo hexane due to the fast combustion process (Elkelawy et al. 2021).

Prepared Lemon grass oil 25% and diesel blend as fuel in that anti-oxidants were added at 500, 1000, 2000 ppm by weight basis and investigated the prepared fuel in the direct injection diesel engine. As a result, butylatedhydroxyanisole had better stability than butylatedhydroxytoluene anti-oxidant additives. But 2000 ppm butylatedhydroxytoluene added to LGO25 showed a significant increase in BTHE, CO, smoke and HC with a decrease in NO<sub>x</sub> emissions of 11%, a decrease in exhaust gas temperature, and a decrease in brake specific fuel consumption compared to lemongrass oil without anti-oxidant additives (R. Sathiyamoorthi and Sankaranarayanan 2016). By feeding the synthesised LGO25, cerium oxide added emulsified LGO25, diethyl ether added emulsified LGO25, and diesel fuel, the combined effect of Nanoemulsion and EGR on performance, emission, and combustion characteristics in a diesel engine was studied. The di ethyl ether added nano emulsified LGO25 with EGR resulted in lower NO<sub>x</sub>, smoke emissions, HC and CO by 30.72%, 11.2%, 18.8% and 33.31%, respectively but increased BTE, BSFC, cylinder pressure and heat release rate by 2.4, 10.8, 4.46 and 3.29% compared to LGO25 as fuel (R. Sathiyamoorthi, Sankaranarayanan, and Pitchandi 2017). Compression ignition engine emission parameters mainly depend on fuel injection and injection pressure timing. CO, HC and smoke emissions decrease and NO<sub>x</sub> increases at the higher injection pressure and advancing injection timing (Sathiyamoorthi and Sankaranarayanan 2016). Small amounts of ethanol in LGO-diesel blends improved LGO25 performance, resulting in an increased cylinder pressure, heat release rate, BSFC, BTE, NO<sub>x</sub>, CO<sub>2</sub>, combustion length and ignition delay time, but lower smoke and HC than diesel and LGO25 (R. Sathiyamoorthi and Sankaranarayanan 2017). Increased injection pressures from 45 to 65 MPa at 50 and 100 Nm of operation with 20 and 50% palm biodiesel resulted in a decrease in BSFC, HC, PM, CO and a little rise in NO<sub>x</sub> emissions in CRDI engines (Algayyim, Wandel, and Yusaf 2018). The effects of the performance and emission behaviour when using various biodiesel feedstock, such as biodiesel from *Jatropha curcas*, Palmyra, Mahua methyl ester, Cashew nut shell and Algae-based biofuel blended with base diesel fuel, have been reported by varying engine influencing input parameters (Senthil kumar and Thirumalini 2020; Prem Anand et al. 2018; Singh et al. 2020a; Prasada Rao and Prasad 2021; Prasada Rao and Prasad 2022; Indrareddy, Venkateswarlu, and Konijeti 2020; Arul Peter et al. 2020; Prakash and Dhanasekaran 2019; Sivaram et al. 2020). A delayed injection reduces emissions without sacrificing performance (Senthil kumar and Thirumalini 2022; Senthil kumar and Thirumalini 2020) (Table 1).

Lemongrass biodiesel's ignition, efficiency and emissions attributes have never been studied in a CRDI engine by adjusting engine input parameters, according to the literature review, to the best of my knowledge. As a result, this research was carried out in a CRDI engine with a data gathering system and an open ECU under atmospheric circumstances, using the RSM design matrix, changing the FIP, FIT, EL, fuel blend and EGR while maintaining a steady rpm of 1500 and a CR of 18. None of the researchers looked into utilising lemongrass biodiesel in a CRDI engine with these input parameters. Finding the best engine operating conditions for diverse fuel sources is also critical for improving the environment and the economy.

**Table 1.** literature survey on parameter optimisation.

Fuel type, blend & ref	Input parameter	Engine details	Optimum parameters	Output responses	Inferences
Linseed oil methyl ester, LOME of 5, 10, 15, 20 & (Manish Kumar et al. 2022)	BLEND, FIP, EGR, LOAD	Kirloskar, VCR, CRDI 1 cylinder, water cooling, 3.5 kW, 1500 RPM, CR = 18, FIT 23°bTDC	5.45% LOME, 57.78 MPa FIP, 6.505% EGR, 6.909 kg load	ITE, NOx increases and HC decreases at all loads	RSM may be used to estimate CRDI engine efficiency and emission parameters while using linseed-based fuel.
Simarouba methyl ester & (Keerthi Kumar et al. 2021)	4.16, 5.2 kW BP load; FIP 205, 220, 240, 260bar; injector hole 3,4,5,6; hole dia 0.2, 0.25, 0.3 mm	TV1, Kirloskar, single cylinder, four stroke, CR = 17.5, 5.2 Kw, 1500 rpm,	6 hole, 240 bar FIP, 0.2 mm hole diameter	BTE increased, HC, CO decreased, NOx marginally increased	Simarouba methyl ester engine's performance was improved by raising the FIP, number of injector holes, and reducing the orifice diameter.
Mahua oil methyl ester, B2OMOME & (Kumar et al. 2019)	Toroid shape piston, FIP 200, 400, 600 bar, FIT 15, 20, 25 bTDC	Kirloskar, VCR, CRDI one cylinder, water-cooling, 3.5 kW@1500 rpm, 661cc, injector holes 6; diameter 0.128 mm	800 bar, 15°bTDC	BTE increased, EGT increased	High injection pressure and fuel injection closer to TDC resulted in better performance.
Pork lard, rape seed oil biodiesel, B60%, B80% & (Duda et al. 2021)	1500, 3000 rpm; 50, 100 & 200 Nm load	ADCR, four-cylinder, capacity 2636 cm <sup>3</sup> , max torque 250Nm	Pork lard biodiesel can be used instead of rape seed biodiesel in terms of performance & emissions.	Biocomponent rich biodiesel based optimisation may be required	The use of alternative fuel has no negative impact on the engine's performance. In medium-duty engines, animal fatty fuel components are a superior alternative to rapeseed methyl ester.
Tallow biodiesel, B20 & (Kanthasamy, Arul Mozhi Selvan, and Shanmugam 2020)	EGR 5, 15, 25%; FIP 400, 500, 600 bar; load 0, 25, 50, 75, 100%; FIT 10, 15, 20°bTDC,	Kirloskar, CRDI, single chamber, water-cooling, CR = 17.5, Power 3.7 kW	600 bar, 25% EGR	CO and smoke decreased	High injection pressure resulted in improved combustion due to better atomisation.
Honge methyl ester, B10, B20, B25 & (S. Kumar and Dinesha 2018)	Blend; EL 50, 75, 100%; CR 16, 17, 18; IT 24,27,30°bTDC	Diesel engine Water cooled, single cylinder, dynamometer load	Load 86.3%; blend 15%; CR 16; IT 26.24°bTDC	BTE 31.5%; NOx 220.6 ppm	BTE is mostly influenced by load, while NOx is influenced by load, CR, and IT. For BTE and NOx, a second order model was created using RSM with a desirability of 0.63. CCD, provides more accurate forecasts than box behnken.
Polanga biodiesel, B0,B10, B20 & (Sharma et al. 2020b)	Blend; FIT 19, 23, 27°bTDC, FIP 160, 180, 200 bar; EL 20, 60,100%	Kirloskar, 4 stroke, DI, water cooled, eddy current dynamometer load; CR 17.5; 5.2 kW @1500 rpm	EL 80%, B23.33%; IT 22.35°bTDC, FIP 192.7 bar	UHC 40.8 ppm; EGT 441.3 K; Pmax 5.53 MPa; BTE 29.55%	Engine input setting can be optimised using the statistical tool of RSM
Nicotianatabacum biodiesel, B0, B10, B20, B30, B40 & (Sharma et al. 2020a)	Blend; EL 20, 40, 60, 80, 100%; FIT 15, 19, 23, 27, 31° bTDC; FIP 16,18,20,22,24MPa	Kirloskar, 4 stroke, DI diesel engine, water cooling, eddy current dynamometer type load, CR 17.5; 5.2 kW at 1500 rpm	EL 45% B30, IP 240 bar, 30°bTDC	BTE 24.1%; HC 39.4 ppm vol.; EGT 479 K; Pmax 4.81MPa	Using RSM, a second order model was created for BTE, HC, Pmax, and EGT with desirability of 0.69.
Moringaoleifera biodiesel, MB50 & (Teoh et al. 2021)	Torque 6.59, 10, 15, 20, 23.41 Nm; SOI 3.625, 5, 7, 9, 10.38 °bTDC; FIP 264, 400, 600, 800, 936 bar; 1000 rpm	Single cylinder, 638cm <sup>3</sup> , CR = 17.7:1, power 7.5 kW @ 2400 rpm, re-entrant type piston	IT 5°bTDC; FIP 400 bar	Higher BTE, NOx and decreased smoke than diesel fuel for all loads of operation for MB50	RSM can be used for the optimisation of engine parameters successfully
Neat lemon grass oil, LGO25 & (Ramalingam et al. 2022)	IP 200, 225, 250; EGR 0, 10, 20; IT 20, 23, 26°bTDC	Kirloskar, 1 cylinder, 4 stroke, DI, air-cooled, stroke 11 cm, bore 8.75 cm, 4.4 kW at 1500 rpm	IP 250bar; IT 26°bTDC; EGR 8.12%	Adding EGR decreases performance, Nox & increases other emissions	RSM is quite helpful in determining the significant factors influencing engine emissions and DOE.

## 2. Materials and methods

Lemongrass can be planted in dryland areas. For plantation, less water is sufficient, it can grow upto 2-metre length, and it has been harvested in three months once. For the experimental analysis, non-consumable Lemongrass oil has been purchased directly from a local vendor in Tamilnadu. It was derived from

grass through a steam distillation process and then converted into biodiesel via a general transesterification process as per ASTM standards; the properties of the prepared biodiesel were compared to baseline diesel, as shown in Table 2. The data indicates that the attributes of processed biodiesel are closer to those of base fuel. Generally, the biodiesel yield depends on the type and amount of catalyst, oil-alcohol ratio, reaction

**Table 2.** Properties of lemongrass biodiesel.

Properties	Unit	Standard diesel	Lemongrass biodiesel	ASTM standard
Acid value	mg of KOH/gm of oil	0.6	0.58	D6751
Free fatty acid	%	0.3	0.29	–
Specific gravity	–	0.816	0.873	D287
Density	kg/m <sup>3</sup>	816	873	D287
Lower calorific value	KJ/kg	42856	39406	D 4809
Higher calorific value	KJ/kg	45309	41855	D 4809
Flash point	°C	53	100	D 93-58T
Fire point	°C	56	103	D 93-58T
Kinematic viscosity @ 40°C	m <sup>2</sup> /s	0.00000209	0.00000391	D445
Dynamic viscosity at 40°C	Pascal second	0.00173	0.00341	D445

temperature, stirring speed, and time is taken to process (Marri, Kotha, and Gaddale 2022) revealed optimum combination of process parameters for getting maximum biodiesel yield of 96.01% vol. by using RSM for *sterculiafoetida* biodiesel such as 26% of methanol ratio, 800 rpm of stir speed, 1.09% of catalyst, 63°C of reaction temperature, and 135 min of reaction time. The raw oil molecule bonding was broken in the transesterification process by adding methanol and catalyst with suitable temperature and agitation-end of the process of alcohol reaction with natural oil obtained, the lemongrass biodiesel and glycerol. Obtained biodiesel was used for experimental work, and the separated glycerol can be used for the pharmaceutical industry. A container was filled with 1 L of raw oil; potassium hydroxide alkaline catalyst of suitable grams. In a separate beaker, appropriate ml of methanol was taken. Potassium hydroxide was mixed with alcohol and stirred until thorough mixing. A mechanical stirrer was used to agitate the raw oil container, while a heating coil was used to heat it simultaneously. The speed of the stirrer was kept to a minimum throughout the initial phases. Once the temperature reached 60 degrees Celsius, the KOH and alcohol solution was poured into the raw oil container and sealed tightly to prevent evaporation during the reaction. Then the air-tight sealed container was stirred at high speed, around 720 rpm, with a constant temperature of 60 degrees Celsius to avoid evaporation. After about two hours of oil-alcohol-catalyst solution stirring at a constant temperature of 60°C, the solution was transferred to a glass container. This container is kept without disturbance for one day to separate biodiesel at the top, and glycerol at the bottom of the vessel. Finally, the glycerol was removed for obtaining the biodiesel after the water wash heat treatment process was repeated until there was no glycerol content in the biodiesel. The image of the prepared biodiesel blend is shown in Figure 1.

### 3. Experimental setup

The experimental work in a single-cylinder, water-cooled, CRDI compressed engine with variable CR is shown in Figure 2. The work was done by changing the fuel sample, fuel injection pressure, fuel injection time, engine load and exhaust gas recirculation rate while maintaining a steady engine rpm of 1500 and a CR of 18. The experimental setup includes all necessary devices for measuring air flow, fuel flow, combustion pressure, crank angle and applied load, as indicated in Table 4. Interfacing using a

high-speed data collecting system, these detected signals are transferred to the computer system. It also comes with a standalone panel box that includes a dual fuel tank, an air box, a manometer, a fuel measuring unit, transmitters, a Piezo powering unit, a rota metre, calorimeters, and a process indicator, among other things. This configuration makes use of a programmable open electronic control unit for fuel injectors, diesel injection, common rail with the rail pressure sensor, pressure regulating valve, crank position measuring sensor, wire harness, and fuel pump, and the accuracy of the instrument used is shown in Table 3. Apex Innovations, Engine soft was used for monitoring the work, reporting, data entry and data logging, as well as processing the various required engine performance and combustion parameters of air–fuel ratio, combustion analysis, heat balance sheet, volumetric efficiency, mechanical efficiency, indicated thermal efficiency, indicated power, fuel flow, Torque, BP, BTE, friction power, indicated mean effective pressure and indicated mean effective pressure. A gas analyser and a smoke metre were also utilised to record contaminants throughout various operating conditions when analysing exhaust emissions. Atmospheric conditions were used for the experiment, and the readings were taken after sufficient time had passed for the system to reach a steady state. Apart from the engine load and exhaust gas recirculation, the remaining activities are monitored and controlled by a Nirai7r-based electronic control unit. In this experiment, 2.5, 4.9, 7.4, 9.8 and 12.3 kg of engine load are represented by 20, 40, 60, 80 and 100% load. For the analysis, water-cooled EGR was achieved by changing the control valve. The intake charge is reduced via cold EGR (Rajesh Kumar and Saravanan 2015) (Tables 3–11).

#### 3.1. Analysis and evaluation of the model

P and F values are mainly generally considered in analysing the developed model. Typically,  $p$  values less than 0.05 as significant. Beyond 0.05, the  $p$ -value is considered insignificant, and the F values above 0.05 are considered favourable. Hence, EL and FB are crucial terms for BMEP and Torque in that aspect. EL and IT are much more significant terms for SFC and the BTE than any other parameters addressed in the investigation. Various engine parameters affecting mechanical efficiency among the different parameters EL, FIT and FB are identified as the most significant. The primary influencing process important parameters for CO pollution are EL, EGR, and FIT, and for NO<sub>x</sub> emissions, they are EGR, IT, IP and FB. ANOVA table for output responses considered indicated in Tables 12 and 13. The regression values found for the analysed output responses of Torque, BMEP, BTE, mechanical efficiency, SFC, CO and NO<sub>x</sub> were 0.99, 0.99, 0.84, 0.98, 0.82, 0.93 and 0.94. Generally, a signal-to-noise ratio of more than 4 is considered preferable. Obtained S/N ratios were 192.180, 190.067, 13.910, 45.646, 13.230, 19.818 and 2.606 for Torque, BMEP, BTE, mechanical efficiency, SFC, CO, NO<sub>x</sub>.

Torque(Nm)

$$= -1.61117 + (0.016275*FB) + (0.233607*EL) \\ + (0.00228806*IP) + (0.0460243*IT) \\ - (0.0239063*EGR) - (4.89583e - 05*(FB*EL))$$



Figure 1. Lemongrass biodiesel blends.



Figure 2. Snapshot of the experimental setup (Manish Kumar et al. 2021a).

**Table 3.** Instrumental uses and accuracy.

Name of device/ instrument	Company/model	Used for	Accuracy
Pressure sensor	PCB Pizotronics USA/M111A22	In cylinder Pressure	−0.01
Analog Temperature Transmitter	WIKA, Pune	Water and exhaust gas temperature	0.50%
Speed Indicator Encoder	Selectron, Mumbai Kubler Germany	RPM indicator Crank angle and RPM	0.05% 0.25%
Dynamometer Load cell	Technomech Sensortronics, Chennai/60001	Loading-Unloading Measure load	0.25% F.S. (0.125 kg)
Load Indicator	ABUS Technologies Inc.	Display applied load	0.2% F.S
Differential Pressure Transmitter	Yokogawa/EJA110A- DMS5A-92NN	Flow rate of fuel	0.10%
Pressure Transmitter	Wika instruments, SL1, Pune	Flow rate of air	0.50%
Rotameter	PG-1–21 Eureka Pune	Flow rate of water	2% F.S.

**Table 4.** Specifications of experimental setup.

Engine components	Specifications
Make	Kirloskar
Type	CRDI VCR engine, single chamber, 4 stroke, water-cooling type, CR (12-18)
Dimensions	Swept length 110 mm, cylinder dia 87.5 mm, swept volume 661.5cm <sup>3</sup> .
Combustion chamber	Hemispherical bowl, connecting rod length 234 mm
Power	3.5 KW @1500 rpm
Compression ratio	18
Load	Eddy current dynamometer type, arm length 185 mm
EGR type	water cooled
ECU Model	Nira i7r sensor injector driver with programmable open ECU software
Piezo sensor	Combustion range 350 bar with low noise cable
Crank angle sensor	Resolution 1°, Speed 5500 RPM with TDC pulse
Data acquisition	NI USB-6210, 16-bit, 250ks/s
Temperature Sensor	RTD Type, PT100, Type K
Load sensor	strain gauge type type, 0–50 Kg
Fuel tank	15 L. Dual compartment
Nozzle	7 Hole & diameter 250 micrometer
Rotameter	Engine cooling 40–400 LPH, Calorimeter 25–250 LPH
Temperature Transmitter	type 2 wire, Input RTD PT 100, Range 0–100°C, output 4–20 mA
Software	Enine soft for performance analysis
Pump	Kirloskar, Monoblock
Setup overall dimension	W2000 X D2500 X H1500

**Table 5.** Accuracy of exhaust measuring device.

Parameters	Measurement	Resolution
CO	0–15% Vol.	0.001%Vol.
NOx	0–5000 ppm Vol.	1 ppm Vol.
Engine speed	400–6000 rpm	1 rpm
Oil temperature	0–125°C	1°C
Lambda	0–9.999	0.001

$$\begin{aligned}
& + (2.08333e - 06(\text{FB}^*\text{IP})) \\
& + (0.000364583(\text{FB}^*\text{IT})) - (0.000505208(\text{FB}^*\text{EGR})) \\
& - (2.60417e - 06(\text{EL}^*\text{IP})) - (0.000164062(\text{EL}^*\text{IT})) \\
& + (1.17188e - 05(\text{EL}^*\text{EGR})) - (8.68056e - 06^*(\text{IP}^*\text{IT})) \\
& - (7.8125e - 06(\text{IP}^*\text{EGR})) + (0.000664063(\text{IT}^*\text{EGR})) \\
& - (0.000215278^*\text{FB}^2) - (2.57812e - 05^*\text{EL}^2)
\end{aligned}$$

**Table 6.** Specifications of exhaust analyser.

Component	Specifications
Device	AVL DIGAS 444N
Display Interface	LCD display USB
Operating Voltage	100–300 V AC
Power consumption	10 W Maximum
Dimensions	270 × 85 × 320 mm

**Table 7.** Summary of responses fit statistics.

Components	Torque (Nm)	BMEP (bar)	BTE (%)	Mech Eff. (%)	SFC (kg/ kWh)	CO in % vol	NOx in PPM vol
$R^2$	0.9993	0.9992	0.8401	0.9875	0.8278	0.9352	0.9454
Adjusted $R^2$	0.9987	0.9987	0.7299	0.9788	0.709	0.8905	0.9077
Predicted $R^2$	0.9975	0.9974	0.452	0.9611	0.3824	0.7862	0.8155
Precision	192.1799	190.0675	13.9104	45.6461	13.2304	19.8178	22.2058

**Table 8.** Summary of various responses model

Response	Source	SS	DF	MS	F-value	p-value	
Torque	Model	806.08	20	40.3	1940.59	< 0.0001	Significant
	Lack of Fit	0.5264	22	0.0239	2.21	0.1429	not significant
BMEP	Model	29.09	20	1.45	1898.13	< 0.0001	Significant
	Lack of Fit	0.0192	22	0.0009	2.05	0.167	not significant
BTE	Model	520.75	20	26.04	7.62	< 0.0001	Significant
	Lack of Fit	96.08	22	4.37	10.1	0.0021	Significant
Mech Eff.	Model	4156.8	20	207.84	114.35	< 0.0001	Significant
	Lack of Fit	41.46	22	1.88	1.17	0.4426	not significant
SFC	Model	0.274	20	0.0137	6.97	< 0.0001	Significant
	Lack of Fit	0.056	22	0.0025	18.77	0.0003	Significant
CO	Model	10.88	20	0.5439	20.92	< 0.0001	Significant
	Lack of Fit	0.6761	22	0.0307	2.76	0.0853	not significant
NOx	Model	7.51E + 06	20	3.75E + 05	25.91	< 0.0001	Significant
	Lack of Fit	3.72E + 05	22	16884.32	2.44	0.1146	not significant

**Table 9.** Constraints and desirability.

Name	Goal	Lower limit	Upper limit	Lower weight	Upper weight	Impor- tance	Desira- bility
A:FB	in range	0	60	1	1	3	1
B:EL	in range	20	100	1	1	3	1
C:IP	in range	400	1000	1	1	3	1
D:IT	in range	6	30	1	1	3	1
E:EGR	in range	0	16	1	1	3	1
Torque (Nm)	maximise	4.61	22.42	1	1	3	0.98
BMEP (bar)	maximise	0.88	4.26	1	1	3	0.98
BTE (%)	maximise	11.7	32.79	1	1	3	0.70
Mech Eff. (%)	maximise	24.59	67.52	1	1	3	0.96
SFC (kg/kWh)	minimise	0.26	0.74	1	1	3	0.89
CO in %	minimise	0.04	0.37	1	1	3	0.72
NOx in PPM	minimise	29	1836	1	1	3	0.84

$$\begin{aligned}
& - (1.56944e - 06^*\text{IP}^2) - (0.00143229^*\text{IT}^2) \\
& + (0.00255859^*\text{EGR}^2)
\end{aligned}$$

BMEP(bar)

$$\begin{aligned}
& = -0.294278 + 0.00291111^*\text{FB} + 0.0444375^*\text{EL} \\
& + 0.000390556^*\text{IP} + 0.00823611^*\text{IT} \\
& - 0.00252083^*\text{EGR} \\
& - 1.04167e - 05^*(\text{FB}^*\text{EL}) + 5.55556e - 07^*(\text{FB}^*\text{IP}) \\
& + 7.63889e - 05^*(\text{FB}^*\text{IT}) - 0.000114583^*(\text{FB}^*\text{EGR}) \\
& - 6.25e - 07^*(\text{EL}^*\text{IP}) - 3.125e - 05^*(\text{EL}^*\text{IT})
\end{aligned}$$

**Table 10.** Input parameters levels.

Name	Units	Factor	Levels				
			-2	-1	0	1	2
FB	%	A	0	15	30	45	60
EL	%	B	20	40	60	80	100
IP	Bar	C	400	550	700	850	1000
IT	bTDC	D	6	12	18	24	30
EGR	%	E	0	4	8	12	16

**Table 11.** Experimental design matrix.

RUN	FB (%)	EL (%)	IP (bar)	IT (bTDC)	EGR (%)
1	30	60	700	18	8
2	45	80	550	24	12
3	45	40	850	12	4
4	45	40	550	24	4
5	45	40	550	24	12
6	45	40	850	24	12
7	15	80	550	12	12
8	45	80	850	12	12
9	45	80	850	12	4
10	15	40	850	24	12
11	30	60	700	18	8
12	45	40	850	24	4
13	45	40	850	12	12
14	15	40	550	12	4
15	45	40	550	12	12
16	45	80	550	24	4
17	30	20	700	18	8
18	30	60	700	18	16
19	30	60	700	18	8
20	15	80	850	24	12
21	15	80	850	12	4
22	45	80	550	12	12
23	45	40	550	12	4
24	30	60	700	18	8
25	30	60	1000	18	8
26	30	60	700	18	8
27	30	60	700	30	8
28	30	100	700	18	8
29	15	40	850	12	4
30	30	60	700	6	8
31	15	80	550	24	4
32	15	80	550	24	12
33	45	80	850	24	12
34	15	40	550	12	12
35	0	60	700	18	8
36	15	40	850	12	12
37	15	40	550	24	12
38	15	80	550	12	4
39	30	60	400	18	8
40	15	40	850	24	4
41	30	60	700	18	8
42	45	80	550	12	4
43	30	60	700	18	8
44	15	80	850	12	12
45	45	80	850	24	4
46	30	60	700	18	8
47	60	60	700	18	8
48	15	40	550	24	4
49	15	80	850	24	4
50	30	60	700	18	0

$$\begin{aligned}
 & - 1.5625e - 05*(EL * EGR) - 6.94444e - 07*(IP*IT) \\
 & - 1.04167e - 06*(IP * EGR) + 0.000104167*(IT * EGR) \\
 & - 3.88889e - 05*FB^2 - 3.125e - 06*EL^2 \\
 & - 2.77778e - 07*IP^2 - 0.000277778*IT^2 \\
 & + 0.00046875 * EGR^2
 \end{aligned}$$

**Table 12.** ANOVA for Torque, BMEP, BTE.

Source	Torque (Nm)		BMEP (bar)		BTE (%)	
	F-value	p-value	F-value	p-value	F-value	p-value
Model	1940.59	< 0.0001	1898.13	< 0.0001	7.62	< 0.0001
A-FB	8.39	0.0071	7.52	0.0104	1.91	0.1777
B-EL	38779.77	< 0.0001	37931.93	< 0.0001	109.46	< 0.0001
C-IP	2.13	0.1553	1.88	0.181	0.0959	0.7591
D-IT	1.88	0.1808	1.88	0.181	9.15	0.0052
E-EGR	2.53	0.1225	2.56	0.1206	0.7026	0.4088

**Table 13.** ANOVA for mechanical efficiency, SFC, CO, NOx.

Source	Mecheff. (%)		SFC (kg/kWh)		CO (%)		NOx (PPM)	
	F-value	p-value	F-value	p-value	F-value	p-value	F-value	p-value
Model	114.35	< 0.0001	6.97	< 0.0001	20.92	< 0.0001	25.91	< 0.0001
A-FB	11.28	0.0022	0.8599	0.3614	0.2224	0.6407	8.64	0.0064
B-EL	2187.75	< 0.0001	94.11	< 0.0001	271.09	< 0.0001	2.19	0.1495
C-IP	0.2532	0.6187	0.3256	0.5726	1.42	0.2437	10.94	0.0025
D-IT	35.09	< 0.0001	4.28	0.0476	23.7	< 0.0001	132.02	< 0.0001
E-EGR	0.0169	0.8973	1.47	0.2351	44.91	< 0.0001	277.60	< 0.0001

BTE (%)

$$\begin{aligned}
 & = -2.71812 + 0.314928*FB + 0.40686*EL \\
 & - 0.00476444*IP + 0.485312*IT \\
 & + 0.263479 * EGR - 0.00239375*(FB*EL) \\
 & - 0.000213611*(FB*IP) - 0.00124306*(FB*IT) \\
 & - 0.00626042*(FB * EGR) + 0.000241458*(EL * IP) \\
 & - 0.00466146*(EL * IT) \\
 & - 0.00653906*(EL * EGR) - 9.375e - 05*(IP*IT) \\
 & + 0.000748958*(IP * EGR) - 0.0276302*(IT * EGR) \\
 & + 0.000396111*FB^2 \\
 & - 0.00179125*EL^2 - 5.01111e - 06*IP^2 \\
 & - 0.000805556*IT^2 + 0.0219375 * EGR^2
 \end{aligned}$$

Mech Eff.(%)

$$\begin{aligned}
 & = 13.1763 - 0.012*FB + 0.723339*EL \\
 & + 0.0132661*IP - 0.43283*IT - 0.451771 * EGR \\
 & + 0.000776042*(FB * EL) - 0.00015375*(FB * IP) \\
 & + 0.00299653*(FB * IT) + 0.00188021*(FB * EGR) \\
 & + 8.05208e - 05*(EL * IP) + 0.00504948*(EL * IT) \\
 & + 0.00195703*(EL * EGR) - 0.000237847*(IP * IT) \\
 & - 0.000224479*(IP * EGR) + 0.0033724*(IT * EGR) \\
 & + 0.000863611*FB^2 - 0.00342516*EL^2 \\
 & - 4.78056e - 06*IP^2 + 0.0108316*IT^2 \\
 & + 0.0229648 * EGR^2
 \end{aligned}$$

SFC (kg/kWh)

$$\begin{aligned}
 & = 0.871403 - 0.00462222*FB - 0.0134521*EL \\
 & + 0.000504444*IP - 0.00720139*IT \\
 & - 0.00795833 * EGR + 4.375e - 05*(FB * EL)
 \end{aligned}$$

$$\begin{aligned}
& + 5.55556e - 07*(FB*IP) + 7.63889e - 05 \\
& *(FB*IT) + 0.000145833*(FB*EGR) \\
& - 5.41667e - 06*(EL*IP) + 6.77083e \\
& - 05*(EL*IT) + 0.00021875*(EL*EGR) \\
& - 2.77778e - 06*(IP*IT) - 1.97917e - 05*(IP*EGR) \\
& + 0.000572917*(IT*EGR) - 8.33333e - 06*FB^2 \\
& + 7.96875e - 05*EL^2 + 2.77778e - 08*IP^2 \\
& + 1.73611e - 05*IT^2 - 0.000507813*EGR^2
\end{aligned}$$

In(CO in % vol)

$$\begin{aligned}
= & -2.71786 + 0.0321448*FB - 0.0127162*EL \\
& + 0.000160862*IP - 0.0842286*IT - 0.0723638 \\
& *EGR - 0.000270825*(FB*EL) - 7.50942e \\
& - 06*(FB*IP) - 6.06494e - 05*(FB*IT) \\
& - 0.000396788*(FB*EGR) - 2.22326e - 05*(EL*IP) \\
& - 0.000218301*(EL*IT) + 0.00126983*(EL*EGR) \\
& + 8.08157e - 05*(IP*IT) + 5.0915e - 05*(IP*EGR) \\
& + 0.000257162*(IT*EGR) - 9.28523e - 05*FB^2 \\
& + 0.000426357*EL^2 - 1.86682e - 07*IP^2 \\
& + 0.00170016*IT^2 + 0.000657658*EGR^2
\end{aligned}$$

NOx

$$\begin{aligned}
= & -601.175 + 30.5422*FB + 12.8991*EL + 0.0124444 \\
& *IP + 14.0788*IT + 67.3938*EGR - 0.112396 \\
& *(FB*EL) - 0.000597222*(FB*IP) \\
& - 0.535069*(FB*IT) + 0.321354*(FB*EGR) \\
& + 0.0161563*(EL*IP) + 0.535677*(EL*IT) \\
& - 1.00664*(EL*EGR) + 0.0342014*(IP*IT) \\
& - 0.0385938*(IP*EGR) - 4.17057*(IT*EGR) \\
& - 0.334139*FB^2 - 0.175141*EL^2 \\
& - 0.000608056*IP^2 + 0.435938*IT^2 \\
& + 0.387109*EGR^2
\end{aligned}$$

### 3.2. Effect of process parameter on torque

All other input components such as fuel blend, FIP, FIT and EGR are less critical than engine load when it comes to Torque. Figure 3(b) shows a 3D surface of Torque versus engine load and injection pressure while maintaining a hold value of 30% fuel blend, injection timing at 18°bTDC, and EGR at 8%. Figure 3(a) shows a 3D surface graph of torque variation versus fuel blend and engine load with the remaining parameters (injection pressure, injection timing, and EGR) set to mid-level hold values. According to the ANOVA table based on the  $P$  value, Torque is primarily influenced by engine load and fuel blend. All other input parameters for the investigation are considered secondary. Because Torque is related to engine load, an increase

in EL will enhance Torque. Figure 3(c) indicates engine loads and their interactive effect on Torque by retaining FIP, EGR and FB as mid-level hold values. Figure 3(d) shows the change of Torque versus engine load, EGR, when the fuel blend is 30%, IP is 700 bar, and injection timing is 18 degrees bTDC. During the experimental investigation, the maximum and minimum Torque obtained was 4.61 and 22.42 Nm, respectively. Advancement of FIT results in improved homogenous air–fuel mixture formation, which supports better combustion quality (Wasiu et al. 2018; Rostami, Ghobadian, and Kiani 2014). Diesel fuel delivered more Torque than biodiesel due to its higher energy content (Igbokwe and Nwafor 2016; Arul Nicholas et al. 2022).

### 3.3. Effect of process parameter on BMEP

The mean pressure developed during the cyclic process is called mean effective pressure. Like Torque, the rising trend of brake mean effective pressure also depends mainly on engine load than on all other parameters considered for the analysis, as shown in Figure 4. It was observed that compared to engine load, the remaining parameter's effect on BMEP was at a minimum level. Increased engine load increased BMEP (Kumar 2021). It is highly related to Torque (Rostami, Ghobadian, and Kiani 2014). The maximum and minimum BMEP obtained during experimental work was 4.26 and 0.88 bar, respectively. When FIP, FIT, and EGR are at mid-level, the variation of EL, and FB effect on BMEP response surface, as shown in Figure 4(a). The FIP and EL effect on BMEP when holding remaining input at the mid-level is shown in Figure 4(b). The impact of FIT and engine load on BMEP when keeping the remaining factor at mid-level is shown in Figure 4(c). The outcome of the EGR and EL effect on BMEP is shown in Figure 4(d) by keeping FB, FIT and FIP at mid-level as hold value. With the use of EGR, the maximum in-cylinder heat release rate was steadily reduced (Ge et al. 2020). Before and after TDC injection experimentation, maximum cylinder pressure was seen at 6°bTDC (Raeie, Emami, and Sadaghiyani 2014). From the ANOVA table based on the  $p$ -value, BMEP mainly depends on engine load and fuel blend than other parameters.

### 3.4. Effect of process parameter on BTE

The 3d surface graph of brake thermal efficiency versus engine load and fuel blend by keeping the remaining parameter at mid-level as shown in Figure 5(a). It has been observed that BTE rises as load increases, a tendency that has also been reported by (M. Kumar et al. 2021b; S. Kumar and Dinesha 2018). The maximum brake thermal efficiency was observed when the engine was operated with 0% bio components in diesel fuel as fuel rather than the increased presence of bio components in diesel fuel for all loads of engine operations. This was due to the reduced energy content of the lemon grass biodiesel. The addition of bio-material in the diesel fuel turns into an increase in density. It decreases the calorific value of supplied energy, causing lower BTE at a full load of engine operations (M. Kumar et al. 2022; M. Kumar et al. 2021b) decrease in thermal efficiency with an increase in blend concentration is due to a rise in viscosity, lower atomisation, and incomplete combustion. Interactive response of FIP, engine load on BTE when holding remaining input factors at mid-level as illustrated in Figure 5(b). The increase in

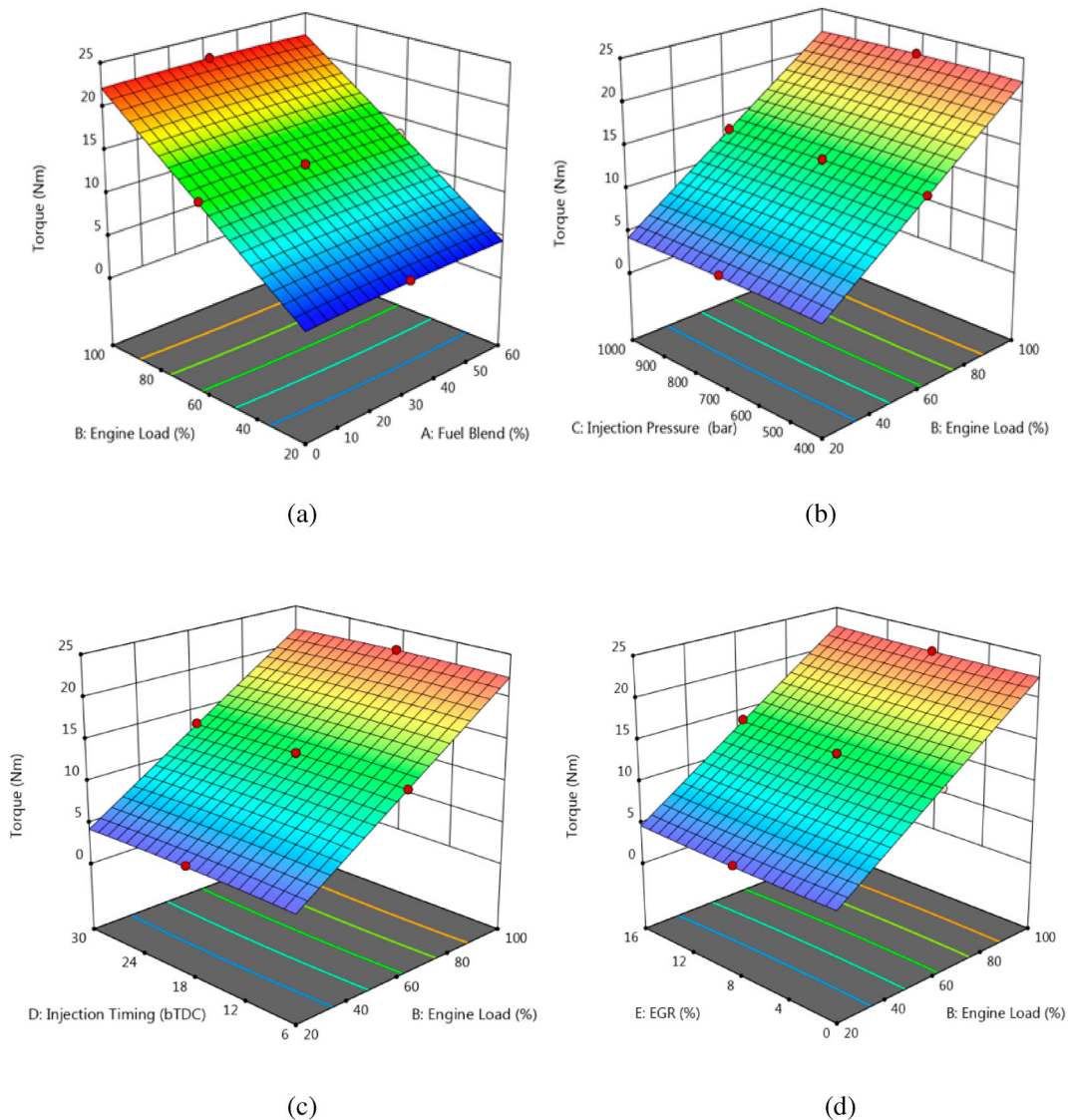


**Figure 3.** 3D surface graph of Torque vs. process parameters.

BTE along with engine load was further increased by increasing the fuel injection pressure minimum of 400 bar to a maximum 1000 bar level of analysis. The injected fuel mixing rate with air at high FIP makes a more delicate spray, and a favourable combustion situation turns into atomisation of fuel spray and better mixing of compressed high pressure, temperature air leads to complete combustion of injected fuel. Maximum brake thermal efficiency was produced at 1000 bar injection pressure and 100% engine load. An increasing trend of BTE was seen by increasing FIP (Manish Kumar et al. 2021b; Dond and Gulhane 2022). The performance of the engine was improved by increasing FIP (Kanthasamy, Arul Mozhi Selvan, and Shanmugam 2020; Kumar et al. 2019; Agarwal et al. 2015; Keerthi Kumar et al. 2021; Arul Nicholas et al. 2022). Advancing the fuel injection timing from 6°bTDC to 30°bTDC and the engine load from 20% to 100%, the brake thermal efficiency output response, as shown in Figure 5(c), by keeping the remaining variable at mid-level as hold values. The maximum brake thermal efficiency was achieved when the fuel was injected nearer to TDC. Significantly

higher BTE was seen when injecting fuel nearer to TDC than advancing (Rostami, Ghobadian, and Kiani 2014; Dond and Gulhane 2022). Throughout the analysis, maximum brake thermal efficiency was achieved at 6°bTDC and engine load at 100% due to maximum brake power, such a trend also observed by (Teoh et al. 2021; Kumar et al. 2019; Dond and Gulhane 2021). An increasing trend of BTHE was seen for retarded FIT upto 10°bTDC for acid oil biodiesel at 600 bar; further, it enhanced upto 900 bar (Rajesh et al. 2018). At high FIP, injecting fuel nearer to TDC gives a favourable combustion situation inside the combustion chamber, but at low injection pressure, injecting fuel too away from TDC provides a good condition, so the optimum combination needs to be analysed (Agarwal et al. 2015). Adding 4, 8, 12, and 16% EGR decreased brake power due to a lack of adequate oxygen inside the combustion chamber, resulting in an unfavourable state for fuel combustion, as illustrated in Figure 5(d). The addition of EGR along with a lower biomaterial fuel blend leads to enhancement in BTE than the addition of EGR along with an increase of fuel blend due to calorific value (N.

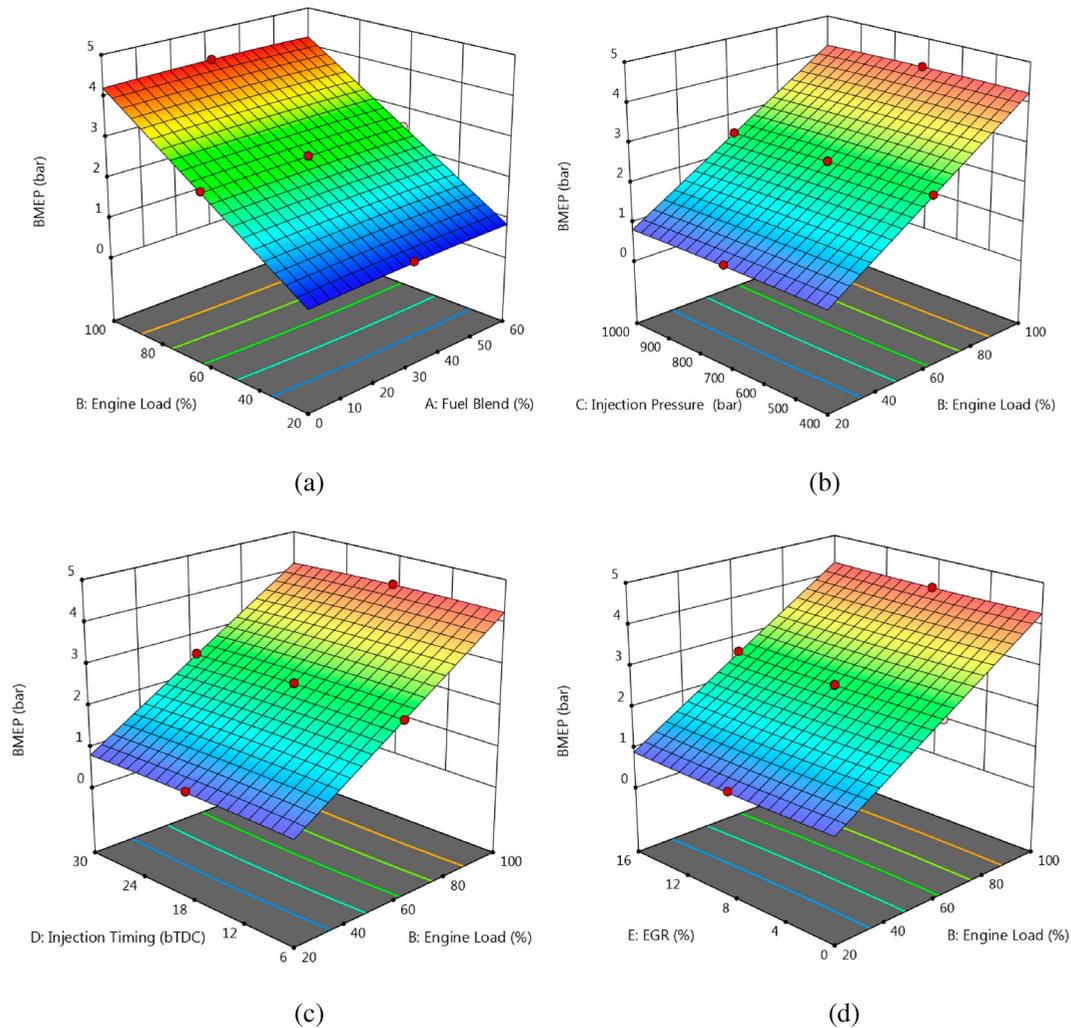


**Figure 4.** 3D surface graph of BMEP vs. process parameters.

Saravanan et al. 2008). Without re-circulating exhaust gas inside the combustion chamber, given higher BTE. The engine's performance marginally decreases EGR's introduction (Rajesh Kumar and Saravanan 2015; Arul Nicholas et al. 2022). An increase in PM and a decrease in efficiency were reported with the addition of EGR (De Serio, de Oliveira, and Sodré 2017). The highest and lowest BTE stands at 11.7% and 32.79% during the experimentation. Maximum BTE has been achieved generally while increasing engine load, decreasing bio-fuel concentration, injecting fuel nearer to TDC, and decreasing EGR. The ANOVA table based on the  $p$ -value shows that the BTE is mainly influenced by engine load and injection timing.

### 3.5. Effect of process parameter on mechanical efficiency

Mechanical efficiency mainly depends on engine load followed by IT and IP than other parameters considered based on significant  $p$ -value in the ANOVA table. Maximum mechanical efficiency was seen by increasing the engine load, IT (too away from TDC), IP and decreasing the EGR, as shown in Figure 4. The variation of mechanical efficiency versus engine load and fuel blend by keeping the remaining input parameter at mid-level, as shown in Figure 6(a). The biomaterial blend increase turns

into a rise in mechanical efficiency, and the maximum mechanical efficiency was seen at the engine operation's high fuel blend and load. The 3d surface responses of injection pressure versus engine load interaction on mechanical efficiency when the remaining input process parameter is kept at mid-level as shown in Figure 6(b). The maximum mechanical efficiency was obtained when the fuel injection pressure and engine load were both high, a tendency also noted by (Manish Kumar et al. 2021b). The variation of mechanical efficiency for FIT versus EL by keeping remaining control factors at mid-level, as shown in Figure 6(c). Injecting the fuel away (6–30 degrees) from before TDC turns into an increasing trend of mechanical efficiency was seen than injection at nearer to before TDC for all loads of engine operations. The maximum and minimum mechanical efficiency are seen when operating the CRDI engine at 30 degree bTDC, 100% of engine load, and at 6 degree of FIT, 20% of engine load. The surface graph variation of mechanical efficiency between EGR and engine load by keeping remaining affecting input factors at mid-level is shown in Figure 6(d). The most excellent and poorest mechanical efficiency during the trial was 67.52 and 24.59%, respectively. Improved performance and emissions of CRDI engine with shorter ignition delay were observed at FIP of 500 bar and 16°bTDC (Marri, Kotha, and Gaddale 2018).

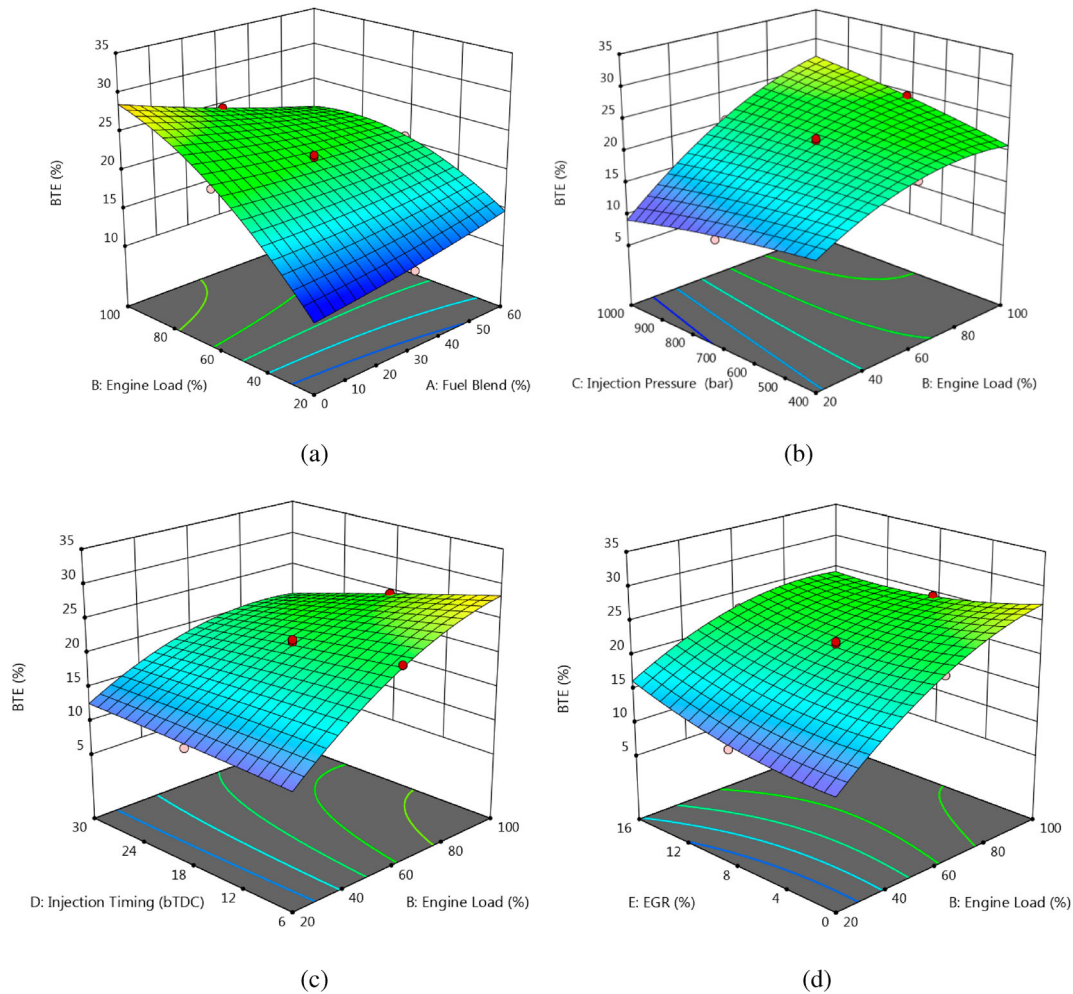
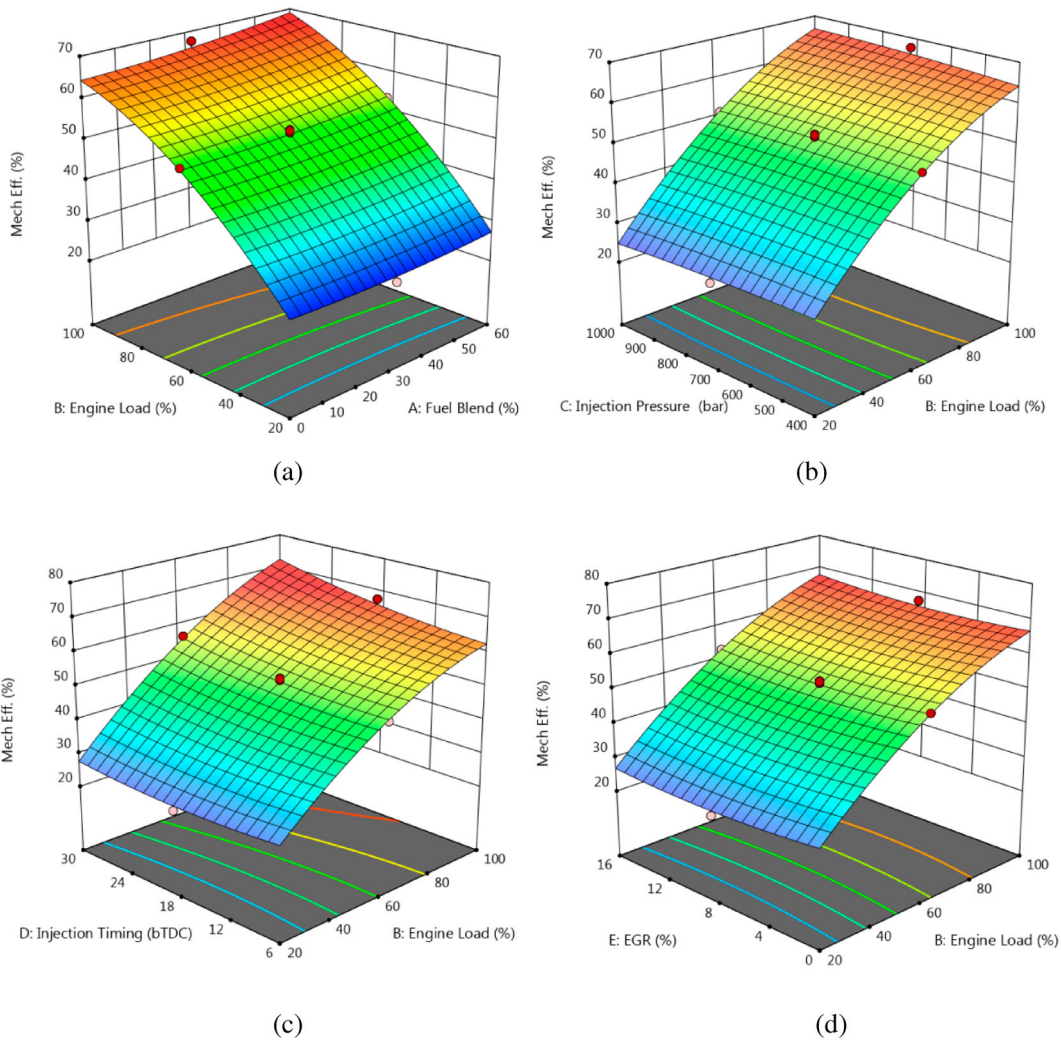


Figure 5. 3D surface graph of BTE vs. process parameters.

### 3.6. Effect of process parameter on SFC

The variation of SFC versus fuel blend and engine load when keeping the remaining input parameter as hold values at the mid-level is illustrated in Figure 7(a). SFC decreased when the load was increased from minimum to maximum for all the test samples. At high engine loads, SFC increases when increasing the bio component in the diesel fuel than pure diesel alone as fuel. But at a low engine operation load, more SFC was observed for pure diesel than biodiesel. The lowest SFC was observed when operating an engine without adding biomaterial in diesel as fuel due to property variations like calorific value and density. Due to the higher heating value of diesel giving better economy than biodiesel blends (Igbokwe and Nwafor 2016; Rostami, Ghobadian, and Kiani Deh Kiani 2014), high mixtures of alcohol lead to an increase in SFC (Siva Prasad, Srinivasa Rao, and Raju 2021). The SFC variation concerning FIP, EL, by considering remaining affecting parameter at a medium level as hold value as shown in Figure 7(b). With increasing FIP, the duration of fuel infusion falls somewhat. Due to the high fuel thickness and lower volatility of biodiesel compared to mineral diesel, a high concentration of biomaterials in test fuel resulted in poor atomisation fuel–air interaction characteristics, which prolonged the combustion duration of biodiesel blends in CRDI engines (Agarwal et al. 2015). When operating the engine at 100% load, SFC drops

with the increase in FIP from 400bar–1000 bar, such a trend also seen by researcher (Yoon, Ge, and Choi 2019; Dond and Gulhane 2021). Advancing fuel injection timing, SFC increases for blended fuel than diesel, as shown in Figure 7(c), by keeping remaining input factors at a medium level. The Lowest SFC was achieved at 6°bTDC and 80% of engine load, advancing fuel injection timing from 6°bTDC to 30°bTDC leads to augmenting in SFC trend was observed as shown in Figure 7(c), retarded FIT gave less SFC than advanced FIT (Dond and Gulhane 2022). At 100% engine load, SFC was increased with the addition of EGR by considering the remaining process parameter at mid-level, as shown in Figure 7(d). The lowest SFC was achieved, operating the engine at 80–90% of engine load, without adding EGR. At the low load of the engine operation, increasing the EGR rate resulted in a drop in SFC than operating an engine without EGR. Still, at the high load of CRDI engine operation, SFC was significantly increased with the addition of the EGR rate (N. Saravanan et al. 2008) without the addition of EGR, the SFC was lower due to lean burn operating conditions. Even with EGR, the BSFC decreases when using the engine at a higher load than a low load (Ge et al. 2020). The lowest and highest SFC of 0.26 and 0.74 kg/kWh were seen throughout the experimental work. Engine load, injection timing, EGR, FB, and IP all play a role in SFC. SFC was reduced during a full load of engine operation by boosting injection pressure



**Figure 6.** 3D surface graph of Mechanical efficiency vs. process parameters.

and lowering fuel IT (i.e. closer to TDC), fuel blend, and EGR addition. The optimum BTHE and BSFC was seen at 100% EL, 10% EGR, 30% fish biodiesel + 0.5% ethyl hexyl nitrate (Karthikeyan et al. 2019).

### 3.7. Effect of process parameter on CO emissions

Figure 8 shows the CO emissions when the effect of any two input factors, such as FB, EL, FIP, FIT and EGR, by keeping the remaining three process parameters at mid-level. Figure 8(a) shows an increase in CO emission with increasing engine load for all experimental blended fuels when the remaining parameters are kept at mid-level as hold values. A decreasing trend of CO emission was seen by increasing FIP, biodiesel concentrations due to proper mixing of air–fuel, higher oxygen content, and complete combustion (Yoon, Ge, and Choi 2019; Dond and Gulhane 2021; Siva Prasad, Srinivasa Rao, and Raju 2021). Increasing the bio-fuel presence in diesel fuel showed a drop of CO emissions, such a trend also seen by (Arul Nicholas et al. 2022). Due to the high oxygen levels in biomaterial, CO pollutants were lower with increasing bio concentration than pure diesel alone at maximum engine operation load. The most elevated CO was measured using petroleum as fuel and operating the engine

at a high load. Increasing the fuel injection pressure from 400 to 1000 bar reduced CO emissions. At maximum engine load, by increasing FIP towards maximum, there was a considerable reduction in CO emissions due to a favourable combustion situation caused by an increase in pressure. A decrease in CO emission was reported by increasing FIP (Kanthasamy, Arul Mozhi Selvan, and Shanmugam 2020; Sathiyamoorthi and Sankaranarayanan 2016). The lowest CO emission was seen at a lower injection pressure of 400 bar and a lower engine load of 20%. Advancing fuel injection timing, i.e. away from TDC, increases CO emission, as shown in Figure 8(c). The maximum CO emission was observed at maximum engine load and FIT at 30°bTDC. The rising trend of carbon monoxide emission was seen by increasing the percentage of EGR addition in the combustion chamber due to the lack of oxygen required for complete combustion, as shown in Figure 8(d); such a trend has also been observed by (Ge et al. 2020). The maximum CO emission was observed at 100% engine load and 16% EGR. At full load, CO emission were tremendously decreased operating engine without addition of EGR (N. Saravanan et al. 2008). The lowest and highest carbon monoxide emissions reported while conducting experimental work were 0.04% and 0.37%. The CO emission mainly depends on EL, EGR, and FIT, followed by FIP and fuel blend in the aspect of  $p$ -value

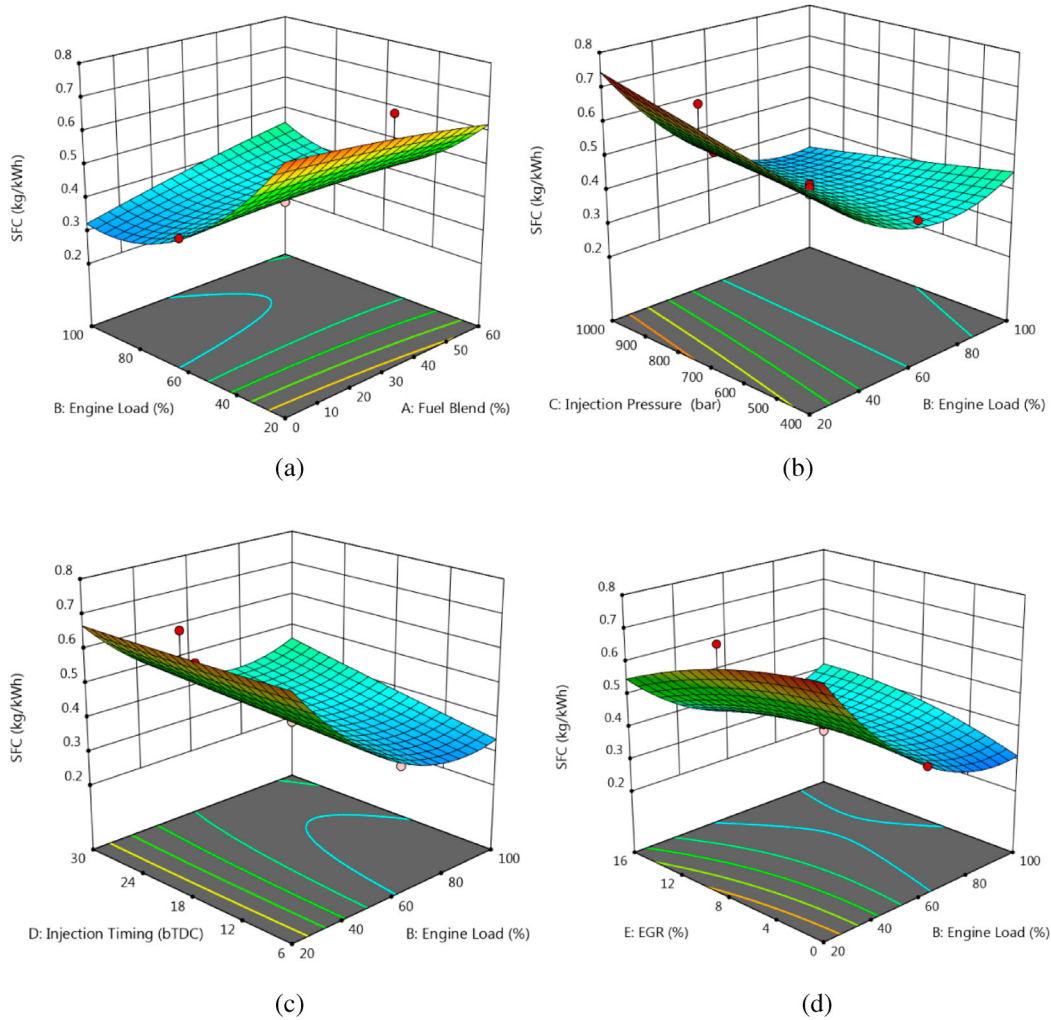


**Figure 7.** 3D surface graph of SFC vs. process parameters.

significance. A decrease in CO emission was seen by increasing the biofuel concentration and FIP and decreasing the IT (injecting fuel nearer to TDC), EGR rate, and engine load. Tables 5 and 6 illustrate the precision and features of exhaust gas analysers. At optimum ternary blends of (cottonseed oil 5% + Mahua 15-20% + n-butanol 15-20%), CO emissions decreased with the expense of HC (Balaji and Veeresh Babu 2022). An increase of ethanol addition in the blends leads to a reduction of NO<sub>x</sub> with the expense of HC and CO (Rajesh et al. 2018).

### 3.8. Effect of process parameter on NO<sub>x</sub>

Figure 9 represents the NO<sub>x</sub> response concerning two input factors while keeping the three influencing parameters at a medium level. An intense increase in NO<sub>x</sub> pollutant emissions was seen by increasing the engine load; such a trend was also seen by (Ge et al. 2020; S. Kumar and Dinesha 2018). A tremendous increase in NO<sub>x</sub> emissions was observed by increasing the engine load from 20% to 100%, and these emissions are reduced significantly by increasing the biodiesel blend. The addition of biodiesel blend up to 30% leads to an increase in NO<sub>x</sub> emissions beyond that level of the addition of biomaterial, emission decreases for all loads of engine operations, as shown in Figure 9(a). The lowest NO<sub>x</sub> was observed at 100% of engine load and 60% of fuel blend

due to low combustion temperature turning into a poor chemical reaction between nitrogen and oxygen components caused by lower calorific value biomaterial than diesel fuel. Maximum NO<sub>x</sub> was observed at 100% of engine load and zero percentage of fuel blends due to high combustion temperature caused by high calorific value diesel fuel. NO<sub>x</sub> pollutant for biodiesel is lesser than diesel (Arul Nicholas et al. 2022). The formation of NO<sub>x</sub> pollutants depends on the product's oxygen content and the ignition temperature. And a slight increase in NO<sub>x</sub> emission was observed by adding a small amount of biodiesel to the supplied fuel; similarly, the same increasing trend of NO<sub>x</sub> was observed by increasing engine load and FIP (Yoon, Ge, and Choi 2019). Increasing FIP from 400 bar to 1000 bar and advancing IT from 6°bTDC to 30°bTDC turns into a tremendous increase in NO<sub>x</sub> emission due to the high FIP and FIT creates enough time for thorough mixing of air-fuel components, leads to a favourable situation for complete combustion turns into high combustion temperature causes nitrogen and oxygen components reactions very vicariously, and lesser ignition delay is shown in Figure 9(c) while keeping remaining input factors at mid-level as hold values. Higher FIP promotes finer spray and atomisation leads to an enhanced mixing rate causes fuel to burn better, resulting in increased thermal efficiency and NO<sub>x</sub> emissions (Agarwal et al. 2015; Siva Prasad, Srinivasa Rao, and Raju 2021). Advancing FIT

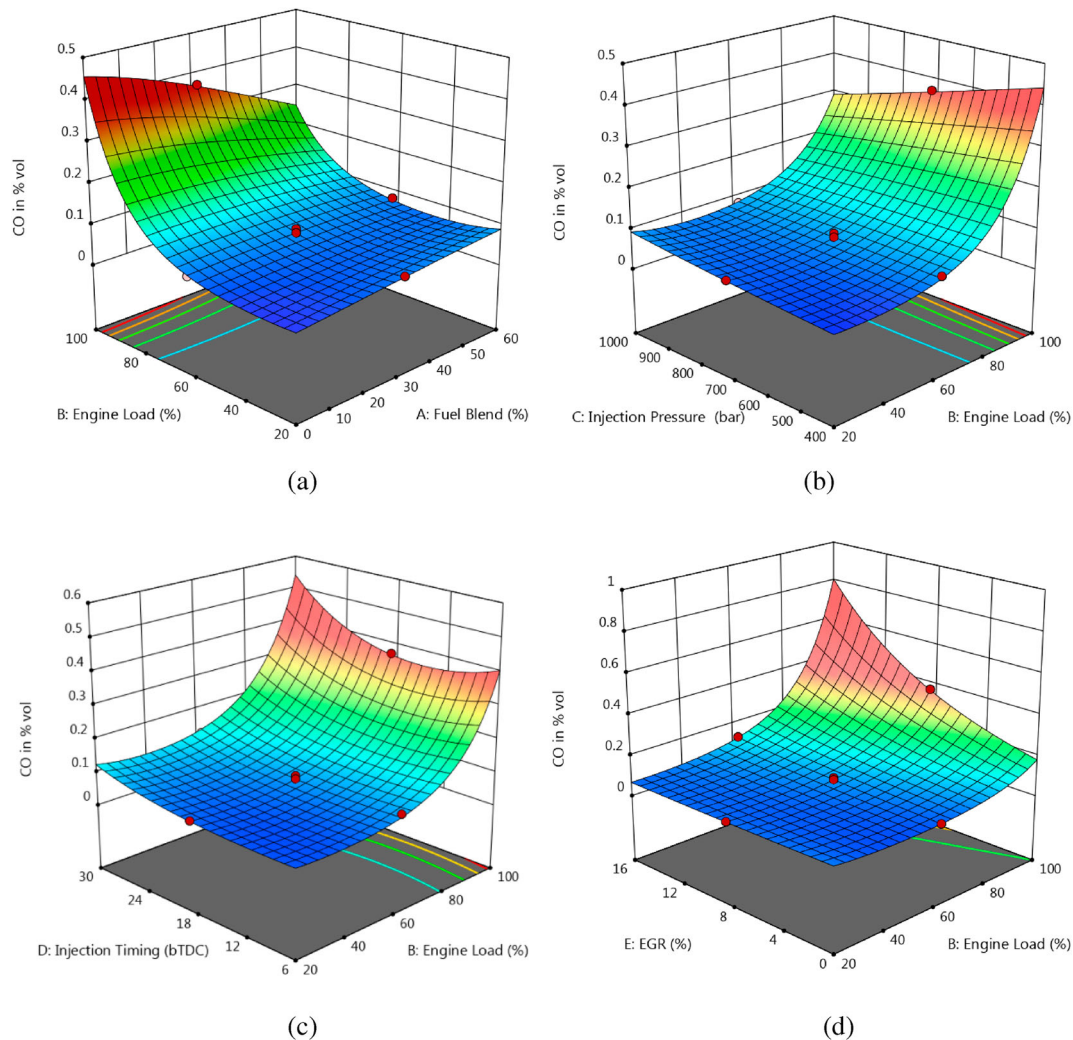


**Figure 8.** 3D surface graph of CO vs. process parameters.

gave higher NO<sub>x</sub> than retarded fuel injection due to decreased delay period and lower combustion temperature (S. Kumar and Dinesha 2018; Marri, Kotha, and Gaddale 2021). At high FIP same trend was seen by (Manish Kumar et al. 2022; Kanthasamy, Arul Mozhi Selvan, and Shanmugam 2020; Marri, Kotha, and Gaddale 2021). Increasing the fuel injection pressure reflects an increase in NO<sub>x</sub> emissions. The maximum NO<sub>x</sub> was observed at 1000 bar, 80% of engine load and the least NO<sub>x</sub> was observed at 400 bar and 100% of engine load. Augmentation trend of NO<sub>x</sub> was observed by advancing fuel injection timing from 6, 12, 18, 24 to 30°bTDC, i.e. away from TDC and maximum NO<sub>x</sub> was observed while injecting fuel at 30°bTDC, at 80% of engine load. Increasing IP, EL turns into an enhancement of NO<sub>x</sub> emissions, as shown in Figure 9(b). Variation of EGR and IT effects on NO<sub>x</sub> is shown in Figure 9(iv). Maximum NO<sub>x</sub> was observed at zero percentage of EGR and injection of fuel too away from TDC of 30°bTDC. An intense decrease of NO<sub>x</sub> emissions was observed with the addition of EGR from 4%, 8%, 12% to 16%, causing lower oxygen presence inside the cylinder to cause incomplete combustion to occur, as shown in Figure 9(d), the such trend also observed by (Ge et al. 2020). The increase of IP from 150 bar to 250 bar results in an increase in the BSFC, HC, CO, NO<sub>x</sub>, smoke density and decreased the BTE, CO<sub>2</sub>, EGT (Elkelawy et al. 2021). The addition

of EGR decreases NO<sub>x</sub> emissions due to lower combustion temperature caused by inert gas inside the cylinder (N. Saravanan et al. 2008). The same trend has been seen in Manish Kumar et al. (2022). NO<sub>x</sub> pollutant mainly depends on EGR, IT, IP, fuel blend followed by Engine load based on the significance of *p*-value. The decreasing trend of NO<sub>x</sub> was seen by increasing the bio-fuel concentration and EGR rate and decreasing the engine load, IP, and IT (nearer to TDC). Smoke and NO<sub>x</sub> levels were reduced in oxygenated blends at the same time (Elkelawy et al. 2018). The primary influencing parameters for managing NO<sub>x</sub> and PM were found as injection timing, CR, EGR and FIP, based on the SN ratio. Because of the high ignition temperature, oxygen concentration, and reaction time in biodiesel-fueled engines, it is recommended to control high ignition temperature using one of two methods: injection of water or emulsion of biodiesel with water, or delayed biodiesel injection of engine operation, which results in a lower reaction time and lower combustion temperature (Fernando, Hall, and Jha 2006). NO<sub>x</sub> emissions for Pongamia biodiesel were lower when the injection was delayed than standard injection (Suryawanshi and Deshpande 2005). As a result, FIT changes have a bigger impact on NO<sub>x</sub> emissions. By delaying FIT by around 2°CA for canola biodiesel, 11% of NO<sub>x</sub> and 2.7% of BSFC were reduced. Engine downsizing, exhaust gas

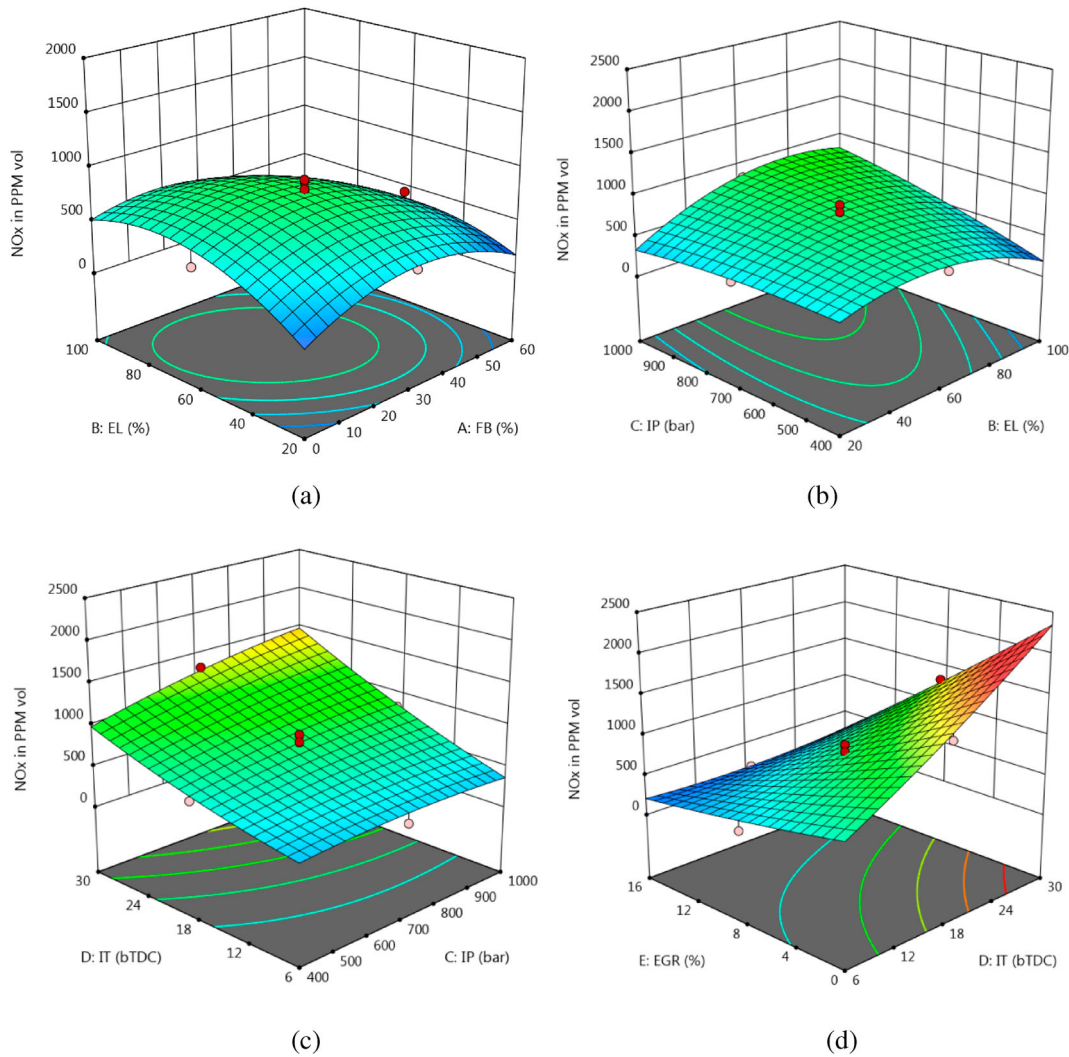


**Figure 9.** 3D surface graph of NOx vs. process parameters.

recirculation and delayed FIT towards TDC are all used to control high NOx levels, and split injection is found to be superior to EGR and delayed injection (Sindhu, Amba Prasad Rao, and Madhu Murthy 2018). At 100% engine load, bsfc and NOx decreased due to a retarding FIT in a heavy-duty diesel engine (Fayad 2019). To identify the best condition, researchers looked at what happened before and after TDC FIT and discovered that early injection produced more NOx than late injection (Raeie, Emami, and Sadaghiyani 2014). For B100, soybean biodiesel gave lower NOx at retarded injection (Qi et al. 2011; Xiao et al. 2020). Using biodiesel and oxygenated additives, researchers varied the FIT (2.5-22.5°bTDC) and EGR (0-30%) and found that injecting closer to TDC resulted in significantly lower NOx than injecting further away. All oxygenated fuels produced less NOx, although the benefit claimed by adding up to 15% EGR on NOx can be accomplished by merely infusing fuel at 2.5°bTDC from 22.5°bTDC. As a result, pumping fuel closer to TDC is more effective than adding EGR for reducing NOx emissions. EGR reduces NOx while significantly increasing CO during full load operation, which is one of the optimisation aims. When utilising rice bran biodiesel without blending with diesel, the key influencing parameter for limiting NOx at no load and part load is EGR. However, FIT is the influencing parameter at full load rather than EGR and FIP (S. Saravanan,

Nagarajan, and Sampath 2013). According to prior studies, even when the engine is operated at full load with B100 alone as fuel and EGR, oxygenated additives, the effect on NOx is mostly managed by injecting fuel closer to TDC; this pattern was also observed in my findings (Gnanasekaran, Saravanan, and Ilangkumaran 2016; Dond and Gulhane 2021). Lower ignition delay due to delayed FIT results in decreased premixed combustion and heat release rate. Retardation also leads to an increase in brake thermal efficiency and a reduction in NOx emissions.

### 3.9. RSM desirability and ANN

In the aspect of fuel injection parameter optimisation in CRDI diesel engines, RSM is an effective approach (Teoh et al. 2021; Saiteja and Ashok 2022; Ramachander et al. 2021). It is an essential tool for multi-objective optimisation of CRDI engines fuelled with linseed biodiesel (Manish Kumar et al. 2021a). Using linseed-based fuel, RSM can predict CRDI engine performance and emission parameters (Manish Kumar et al. 2022). Engine input setting can be optimised using a statistical tool of RSM (Sharma et al. 2020b; Sharma et al. 2020a; Teoh et al. 2021; Ramalingam et al. 2022). Hence, it is clear that the RSM tool can be used for designing the experiment and analysing

multi-objective problems, prediction and optimisation. Bio-component-rich biodiesel based optimisation is required (Duda et al. 2021). CCD comparatively gives accurate predictions (S. Kumar and Dinesha 2018). Experimental work was conducted based on a central composite design matrix. And using the obtained experimental data, the numerical multi-objective optimisation was carried out using an RSM optimiser to know the level of desirability with the objective of minimising the output responses of specific fuel consumption, carbon monoxide, oxides of nitrogen and maximising the responses of torque, and brake mean effective pressure, brake thermal efficiency and mechanical efficiency by maintaining equal importance or weightage to all the response factor. The individual desirability of 0.98, 0.98, 0.70, 0.965, 0.89, 0.70, 0.85 for torque, brake mean effective pressure, brake thermal efficiency, mechanical efficiency, specific fuel consumption, carbon monoxide, oxides of nitrogen were shown in Table 9. Maximum desirability of 0.863 was seen out of 100 solutions by increasing engine load (20% to 100%), increasing fuel blend (0–60%), increasing injection pressure (400 bar to 1000 bar), injecting fuel nearer to TDC (30°bTDC to 6°bTDC) and decreasing exhaust gas recirculation (16–0%).

To validate RSM analysis, experimental work was conducted at RSM predicted optimum combinations three times, and the error was within the level of acceptance, as shown in Table 14. The RSM optimised result to meet goals was 59.991%, 99.984%, 999.9 bar, 6°bTDC and 0.008% of FB, EL, IP, IT and EGR, respectively.

Levenberg-Marquardt backpropagation algorithm model developed For predicting output response one by one, MATLAB R2019b was utilised. The following steps were taken: load data, partition data into input and output, define network structure, train and test the network by modifying hidden layer size until appropriate regression values were obtained, lastly, error calculation between target and output, and graph presentation. The ANN technique can be more accurately forecast process output responses than RSM-based prediction. Table 15 shows the calculated regression values of ANN with hidden layer size and iterations for CRDI engine performance parameters of mechanical efficiency, BTE, SFC and CO, NOx emission parameters.

**Table 14.** RSM predicted VS experimental values.

Components	Predicted	Experimental	Error (%)
FB (%)	59.991	60	
EL (%)	99.984	100	
IP (bar)	999.992	1000	
IT (°bTDC)	6	6	
EGR (%)	0.008	0	
Torque (Nm)	22.184	21.783	1.81
BMEP (bar)	4.217	4.138	1.87
BTE (%)	26.642	26.122	1.95
Mech Eff. (%)	66.085	65.601	0.73
SFC (kg/kWh)	0.311	0.321	3.22
CO in % vol	0.078	0.080	2.56
NOx in PPM vol	310.674	317.333	2.14

**Table 15.** ANN regression

	Mech. efficiency	BTE	SFC	CO	NOx
R (ANN)	0.99425	0.90405	0.93853	0.97169	0.95377
Hidden layer	5	32	5	10	7
Iterations	21	5	12	10	14
R <sup>2</sup> (RSM)	0.9875	0.8401	0.8278	0.9352	0.9454

## 4. Conclusions

RSM optimiser was used to optimise parameters of a single cylinder 4 strokes, water cooling type CRDI compressed ignition engine based on a design matrix by varying the blends of lemon grass biodiesel, engine load, FIP, FIT and EGR up to 16%. An ANOVA analysis was conducted to discover the major influencing input components on output responses.

For forecasting torque, BMEP, mechanical efficiency, BTE, BSFC, CO and NOx, RSM was utilised to build a second-order polynomial quadratic model. In addition, there was no discernible discrepancy between fitted values and experimental data. RSM was verified by performing experimental work at the best possible combination, and the error was within acceptable bounds.

The impact of engine load and biodiesel blend on torque and BMEP output responses is stronger than the rest of the parameters evaluated.

The effects of engine load and injection timing on brake thermal efficiency and specific fuel usage are more potent than other variables evaluated.

The impact of engine load, injection time, and fuel blend on mechanical efficiency is greater than the impact of the other characteristics evaluated.

CO emissions are influenced more by engine load, injection time and exhaust gas recirculation than by fuel blend and injection pressure.

NOx emissions are influenced by exhaust gas recirculation, injection timing, injection pressure and fuel blend, followed by engine load.

Based on the desirability method, the best process parameter for highest performance and least emissions is 12.3 kg of engine load, 60% biodiesel blend, 1000 bar injection pressure, 6°bTDC, and without the addition of EGR.

ANN predicts mechanical efficiency, BTE, SFC, CO and NOx to be 0.68, 7.6, 13.3, 3.90 and 0.88% higher than RSM.

When the input configuration is 15% of blends, 80% of EL, 850bar of FIP, 12°bTDC of FIT, and 12% of EGR, the minimum indicated BSFC and maximum BTHE are 0.26 kg/KW.hr and 32.79%, respectively. The settings of 30% mixes, 20% EL, 700 bar FIP, 18°bTDC of FIT, and 8% EGR has been reported to have maximum BSFC and minimum BTHE of 0.74 kg/KW.hr and 11.7%, respectively.

Lemongrass biodiesel can be used as an alternative fuel in CRDI engines, according to a feasibility study of high percentage lemongrass biodiesel blends conducted at varied retarded FIT and FIP up to 1000 bar.

According to the results of the ANOVA study, EL has a 99% influence on BMEP and torque. EL's impact on BTHE is 60.3%. EL influences 94.4% of mechanical efficiency. EL has a 55.9% sway over SFC. EL, EGR and IT respectively influence CO by 60.58%, 10% and 5.3%. EGR and IT both have a 50.5% and 23.9% impact on NOx.

This optimised result is only appropriate for the 1500 rpm and 18:1 compression ratio of the CRDI engine parameters that were investigated in the investigation.

## Disclosure statement

No potential conflict of interest was reported by the author(s).

## ORCID

Paramasivam Prakash  <http://orcid.org/0000-0003-4711-4868>

## References

- Agarwal, Avinash Kumar, Atul Dhar, Jai Gopal Gupta, Woong Il Kim, Kibong Choi, Chang Sik Lee, and Sungwook Park. 2015. "Effect of Fuel Injection Pressure and Injection Timing of Karanja Biodiesel Blends on Fuel Spray, Engine Performance, Emissions and Combustion Characteristics." *Energy Conversion and Management* 91 (February): 302–314. doi:10.1016/j.enconman.2014.12.004.
- Algayyim, Sattar Jabbar Murad, Andrew P. Wandel, and Talal Yusaf. 2018. "The Impact of Injector Hole Diameter on Spray Behaviour for Butanol-Diesel Blends." *Energies* 11(5): 1–12. 1298. doi:10.3390/EN11051298.
- Arul Nicholas, T., A. Venkatakrisna, Nivin Joy, and Anish Mariadhas. 2022. "Performance and Emission Analysis on Diesel Engine Fuelled with Neat Pongamia Biodiesel." *International Journal of Ambient Energy* 43 (1): 21–27. doi:10.1080/01430750.2019.1630315.
- Arul Peter, A., M. Chandrasekaran, P. Prakash, T. Vinod Kumar, and P. Vivek. 2020. "Experimental Investigation of a Spark Ignition Engine Using Blends of Biogas." *International Journal of Ambient Energy* 41 (4): 462–465. doi:10.1080/01430750.2018.1472656.
- Balaji, Bhukya, and A. Veeresh Babu. 2022. "Experimental Investigation of a Novel Quaternary Blend for CRDI Engine: Performance, Emission, and Combustion Characteristics." *Energy Sources, Part A: Recovery, Utilization and Environmental Effects* 44 (3): 5729–5754. doi:10.1080/15567036.2022.2087803.
- Caballero-Gallardo, Karina, Dalila Rodriguez-Niño, Katerin Fuentes-Lopez, Elena Stashenko, and Jesus Olivero-Verbel. 2021. "Chemical Composition and Bioactivity of Essential Oils from *Cymbopogon Nardus* L. and *Rosmarinus Officinalis* L. Against Ulomoides Dermestoides (Fairmaire, 1893) (Coleoptera: Tenebrionidae)." *Journal of Essential Oil-Bearing Plants* 24 (3): 547–560. doi:10.1080/0972060X.2021.1936205.
- Chandra Sekhar, S., K. Karuppasamy, N. Vedaraman, A. E. Kabeel, Ravishankar Sathyamurthy, Medhat Elkelay, and Hagar Alm Eldin Bastawissi. 2018. "Biodiesel Production Process Optimization from *Pithecellobium Dulce* Seed Oil: Performance, Combustion, and Emission Analysis on Compression Ignition Engine Fuelled with Diesel/Biodiesel Blends." *Energy Conversion and Management* 161 (November 2017): 141–154. doi:10.1016/j.enconman.2018.01.074.
- De Serio, Domenico, Alex de Oliveira, and José Ricardo Sodr . 2017. "Effects of EGR Rate on Performance and Emissions of a Diesel Power Generator Fueled by B7." *Journal of the Brazilian Society of Mechanical Sciences and Engineering* 39 (6): 1919–1927. doi:10.1007/S40430-017-0777-X/FIGURES/10.
- Dond, Dipak Kisan, and Nitin Parashram Gulhane. 2021. "Optimization of Injection System Parameter for CRDI Small Cylinder Diesel Engine by Using Response Surface Method." *Journal of The Institution of Engineers (India): Series C* 102 (4): 1007–1029. doi:10.1007/s40032-021-00688-6.
- Dond, Dipak Kisan, and Nitin P Gulhane. 2022. "Optimization of Combustion Parameters for CRDI Small Single Cylinder Diesel Engine by Using Response Surface Method." *Journal of Mechanical Engineering and Sciences* 16 (1): 8730–8742. doi:10.15282/jmes.16.1.2022.07.0690.
- Duda, Kamil, Sławomir Wierzbicki, Maciej Mikulski, Łukasz Konieczny, Bogusław Łazarz, and Magdalena Letuń-Łątka. 2021. "Emissions from a Medium-Duty Crdi Engine Fuelled with Diesel-Biodiesel Blends." *Transport Problems* 16 (1): 39–49. doi:10.21307/tp-2021-004.
- Elkelawy, Medhat, Hagar Alm-Eldin Bastawissi, E. A. El Shenawy, Mohammed Taha, Hitesh Panchal, and Kishor Kumar Sadasivuni. 2021a. "Study of Performance, Combustion, and Emissions Parameters of DI-Diesel Engine Fueled with Algae Biodiesel/Diesel/n-Pentane Blends." *Energy Conversion and Management: X* 10: 100058. doi:10.1016/j.ecmx.2020.100058.
- Elkelawy, Medhat, Hagar Alm-Eldin Bastawissi, Khaled Khodary Esmaeil, Ahmed Mohamed Radwan, Hitesh Panchal, Kishor Kumar Sadasivuni, Deepalekshmi Ponnamma, and Rashmi Walvekar. 2019. "Experimental Studies on the Biodiesel Production Parameters Optimization of Sunflower and Soybean Oil Mixture and DI Engine Combustion, Performance, and Emission Analysis Fuelled with Diesel/Biodiesel Blends." *Fuel* 255 (July): 115791. doi:10.1016/j.fuel.2019.115791.
- Elkelawy, Medhat, Hagar Alm Eldin Bastawissi, Khaled Khodary Esmaeil, Ahmed Mohamed Radwan, Hitesh Panchal, Kishor Kumar Sadasivuni, Muthusamy Suresh, and Mohammad Israr. 2020a. "Maximization of Biodiesel Production from Sunflower and Soybean Oils and Prediction of Diesel Engine Performance and Emission Characteristics Through Response Surface Methodology." *Fuel* 266 (December 2019): 117072. doi:10.1016/j.fuel.2020.117072.
- Elkelawy, Medhat, Hagar Bastawissi, Ravishankar Sathyamurthy, S. Chandra Sekar, K. Karuppasamy, N. Vedaraman, and Karuppiah Sathiyamoorthy. 2018. "Numerical and Experimental Investigation of Ethyl Alcohol as Oxygenator on the Combustion, Performance, and Emission Characteristics of Diesel/Cotton Seed Oil Blends in Homogenous Charge Compression Ignition Engine." *SAE Technical Papers* 2018-Septe (September): 1–13. doi:10.4271/2018-01-1680.
- Elkelawy, Medhat, E. A. El Shenawy, Salma khalaf Abd Almonem, M. H. Nasef, Hitesh Panchal, Hagar Alm Eldin Bastawissi, Kishor Kumar Sadasivuni, Akhilesh Kumar Choudhary, Deepak Sharma, and Mohammad Khalid. 2021b. "Experimental Study on Combustion, Performance, and Emission Behaviours of Diesel/WCO Biodiesel/Cyclohexane Blends in DI-CI Engine." *Process Safety and Environmental Protection* 149. Institution of Chemical Engineers: 684–697. doi:10.1016/j.psep.2021.03.028.
- Elkelawy, Medhat, Safaa El din H. Etaiw, Hagar Alm-Eldin Bastawissi, Mohamed I. Ayad, Ahmed Mohamed Radwan, and Mohamed M. Dawood. 2021c. "Diesel/ Biodiesel /Silver Thiocyanate Nanoparticles/Hydrogen Peroxide Blends as New Fuel for Enhancement of Performance, Combustion, and Emission Characteristics of a Diesel Engine." *Energy* 216: 119284. doi:10.1016/j.energy.2020.119284.
- Elkelawy, Medhat, Safaa El din H. Etaiw, Hagar Alm Eldin Bastawissi, Hassan Marie, Ahmed Elbanna, Hitesh Panchal, Kishorkumar Sadasivuni, and Hitesh Bhargav. 2020b. "Study of Diesel-Biodiesel Blends Combustion and Emission Characteristics in a CI Engine by Adding Nanoparticles of Mn (II) Supramolecular Complex." *Atmospheric Pollution Research* 11 (1): 117–128. doi:10.1016/j.apr.2019.09.021.
- Fayad, Mohammed A. 2019. "Effect of Fuel Injection Strategy on Combustion Performance and NOx/Smoke Trade-off Under a Range of Operating Conditions for a Heavy-Duty DI Diesel Engine." *SN Applied Sciences* 1 (9): 1–10. doi:10.1007/S42452-019-1083-2/FIGURES/8.
- Fernando, Sandun, Chris Hall, and Saroj Jha. 2006. "NOx Reduction from Biodiesel Fuels." *Energy and Fuels* 20 (1): 376–382. doi:10.1021/EF050202M.
- Ganesan, S., J. Senthil Kumar, and J. Hemanandh. 2020. "Optimisation of CI Engine Parameter Using Blends of Biodiesel by the Taguchi Method." *International Journal of Ambient Energy* 41 (2): 205–208. doi:10.1080/01430750.2018.1456968.
- Ge, Jun Cong, Ho Young Kim, Sam Ki Yoon, and Nag Jung Choi. 2020. "Optimization of Palm Oil Biodiesel Blends and Engine Operating Parameters to Improve Performance and PM Morphology in a Common Rail Direct Injection Diesel Engine." *Fuel* 260 (January), doi:10.1016/J.FUEL.2019.116326.
- Gnanasekaran, Sakthivel, N. Saravanan, and M. Ilankumaran. 2016. "Influence of Injection Timing on Performance, Emission and Combustion Characteristics of a DI Diesel Engine Running on Fish Oil Biodiesel." *Energy* 116 (December): 1218–1229. doi:10.1016/J.ENERGY.2016.10.039.
- Igbokwe, J. O., and O. M. I. Nwafor. 2016. "Performance Characteristics of Palm Kernel Biodiesel and Its Blend in a CI Engine." *International Journal of Ambient Energy* 37 (1): 103–106. doi:10.1080/01430750.2014.897647.
- Indrareddy, N., K. Venkateswarlu, and Ramakrishna Konijeti. 2020. "Experimental Investigation of Algae Biofuel–Diesel Blends on Performance of a CRDI Diesel Engine." *International Journal of Ambient Energy*. doi:10.1080/01430750.2020.1725630.
- Kanthasamy, P., V. Arul Mozhi Selvan, and P. Shanmugam. 2020. "Investigation on the Performance, Emissions and Combustion Characteristics of CRDI Engine Fueled with Tallow Methyl Ester Biodiesel Blends with Exhaust Gas Recirculation." *Journal of Thermal Analysis and Calorimetry* 141 (6): 2325–2333. doi:10.1007/s10973-020-09770-0.
- Karthikeyan, Rajagopalan, Kavati Venkateswarlu, Syed Yousufuddin, and A. Punitha. 2019. "Regression and Taguchi – Gray Analysis for Multi Response Optimization of Alternative Fuel Operated Diesel Engine with EGR." *Energy Sources, Part A: Recovery, Utilization, and Environmental Effects*. doi:10.1080/15567036.2019.1683101.

- Keerthi Kumar, N., N. R. Banapurmath, T. K. Chandrashekar, G. S. Jatadhara, Manzoore Elahi M. Soudagar, Ali E. Anqi, M. A. Mujtaba, et al. 2021. "Effect of Parameters Behavior of Simarouba Methyl Ester Operated Diesel Engine." *Energies* 14 (16): 4973. doi:10.3390/en14164973.
- Kumar, Manish, Naushad Ahmad Ansari, Abhishek Sharma, V. K. Singh, Raghvendra Gautam, and Yashvir Singh. 2021a. "Prediction of an Optimum Engine Response Based on Different Input Parameters on Common Rail Direct Injection Diesel Engine: A Response Surface Methodology Approach." *Scientia Iranica* 28 (6): 3181–3200. doi:10.24200/sci.2021.56745.4885.
- Kumar, Manish, Naushad Ahmad Ansari, Abhishek Sharma, Varun Kumar Singh, Raghvendra Gautam, and Yashvir Singh. 2021b. "Prediction of an Optimum Engine Response Based on Various Input Parameters on Common Rail Direct Injection Diesel Engine- A Response Surface Methodology Approach." *Scientia Iranica* 28 (6): 0–0. doi:10.24200/sci.2021.56745.4885.
- Kumar, M., N. A. Ansari, A. Sharma, V. K. Singh, R. Gautam, and Y. Singh. 2021. "Prediction of an Optimum Engine Response Based on Different Input Parameters on Common Rail Direct Injection Diesel Engine: A Response Surface Methodology Approach." *Scientia Iranica* 28 (6): 3181–3200. doi:10.24200/SCI.2021.56745.4885.
- Kumar, Prashanth, Nagaraj R. Banapurmath, Peter Fernandes, and K. Raju. 2019. "Influence of Injection Strategy on B20MOME Fueled CRDI Engine with Toroid Shaped Piston Cavity." *European Journal of Sustainable Development Research* 3(3): em0086. doi:10.20897/ejosdr/3974.
- Kumar, Shiva, and P. Dinesha. 2018. "Optimization of Engine Parameters in a Bio Diesel Engine Run with Honge Methyl Ester Using Response Surface Methodology." *Measurement: Journal of the International Measurement Confederation* 125 (September): 224–231. doi:10.1016/j.measurement.2018.04.091.
- Kumar, Manish, Varun Kumar Singh, Abhishek Sharma, Naushad Ahmad Ansari, Raghvendra Gautam, and Yashvir Singh. 2022. "Effect of Fuel Injection Pressure and EGR Techniques on Various Engine Performance and Emission Characteristics on a CRDI Diesel Engine When Run with Linseed Oil Methyl Ester." *Energy and Environment* 33 (1): 41–63. doi:10.1177/0958305X20983477.
- Kumar, Niraj, Varun, and Sant RamChauhan. 2013. "Performance and Emission Characteristics of Biodiesel from Different Origins: A Review." *Renewable and Sustainable Energy Reviews* 21: 633–658. doi:10.1016/j.rser.2013.01.006.
- Marri, Vinod Babu, Madhu Murthy Kotha, and Amba Prasad Rao Gaddale. 2018. "Experimental Investigations on the Influence of Higher Injection Pressures and Retarded Injection Timings on a Single Cylinder CRDI Diesel Engine." *International Journal of Ambient Energy* 42 (4): 444–457. doi:10.1080/01430750.2018.1540017.
- Marri, Vinod Babu, Madhu Murthy Kotha, and Amba Prasad Rao Gaddale. 2021. "Experimental Investigations on the Influence of Higher Injection Pressures and Retarded Injection Timings on a Single Cylinder CRDI Diesel Engine." *International Journal of Ambient Energy* 42 (4): 444–457. doi:10.1080/01430750.2018.1540017.
- Marri, Vinod Babu, Madhu Murthy Kotha, and Amba Prasad Rao Gaddale. 2022. "Production Process Optimisation of Sterculia Foetida Methyl Esters (Biodiesel) Using Response Surface Methodology." *International Journal of Ambient Energy* 43 (1): 1837–1846. doi:10.1080/01430750.2020.1723692.
- Mukarram, Mohammad, Sadaf Choudhary, Mo Ahamad Khan, Palmiro Poltronieri, M. Masroor A, Jamin Ali Khan, Daniel Kurjak, and Mohd Shahid. 2022. "Lemongrass Essential Oil Components with Antimicrobial and Anticancer Activities." *Antioxidants* 11(1). doi:10.3390/antiox11010020.
- Narayanan, S., K. Ramesh, and R. Sakthivel. 2019. "Optimization of Nozzle Hole Number for a Diesel Engine Fueled with Kapok Methyl Ester Blend." *Energy Sources, Part A: Recovery, Utilization, and Environmental Effects*. October. Taylor and Francis Inc, 1–13. doi:10.1080/15567036.2019.1675817.
- Prakash, P., and C. Dhanasekaran. 2019. "Experimental Investigation on Jatropa-Methanol Blends in Direct Injection Diesel Engines." *International Journal of Vehicle Structures and Systems* 11 (3): 290–293. doi:10.4273/ijvss.11.3.14.
- Prasada Rao, Geddam, and L. S. V. Prasad. 2021. "An Attempt for Improving the Performance, Combustion and Exhaust Emission Attributes of an Existing Unmodified Diesel Engine Powered with Palmyra Biodiesel Blends." *International Journal of Ambient Energy* 43 (1): 4424–4432. doi:10.1080/01430750.2021.1907618.
- Prasada Rao, Geddam, and Lankapalli Sathya Vara Prasad. 2022. "Combined Influence of Compression Ratio and Exhaust Gas Recirculation on the Diverse Characteristics of the Diesel Engine Fueled with Novel Palmyra Biodiesel Blend." *Energy Conversion and Management: X* 14 (May): 100185. doi:10.1016/j.ecmx.2022.100185.
- Prem Anand, B., S. Prasanna Raj Yadav, B. Aasthiya, G. Akshaya, and K. Arulmozhi. 2018. "Effect of Fuel Injection Strategies on the Performance of the Common Rail Diesel Injection (CRDI) Engine Powered by Biofuel." *International Journal of Ambient Energy* 41 (14): 1577–1586. doi:10.1080/01430750.2018.1517690.
- Qi, Donghui, Michael Leick, Yu Liu, and Chia Fon F. Lee. 2011. "Effect of EGR and Injection Timing on Combustion and Emission Characteristics of Split Injection Strategy DI-Diesel Engine Fueled with Biodiesel." *Fuel* 90 (5): 1884–1891. doi:10.1016/J.FUEL.2011.01.016.
- Raeie, Nader, Sajjad Emami, and Omid Karimi Sadaghiyani. 2014. "Effects of Injection Timing, Before and After Top Dead Center on the Propulsion and Power in a Diesel Engine." *Propulsion and Power Research* 3 (2): 59–67. doi:10.1016/J.JPPR.2014.06.001.
- Rajesh, S., B. M. Kulkarni, N. R. Banapurmath, and S. Kumarappa. 2018. "Effect of Injection Parameters on Performance and Emission Characteristics of a CRDI Diesel Engine Fueled with Acid Oil Biodiesel-Ethanol Blended Fuels." *Biofuels* 9 (3): 353–367. doi:10.1080/17597269.2016.1271628.
- Rajesh Kumar, B., and S. Saravanan. 2015. "Effect of Exhaust Gas Recirculation (EGR) on Performance and Emissions of a Constant Speed DI Diesel Engine Fueled with Pentanol/Diesel Blends." *Fuel* 160 (November): 217–226. doi:10.1016/j.fuel.2015.07.089.
- Ramachander, J., S. K. Gugulothu, G. R. K. Sastry, Jibitesh Kumar Panda, and M. Siva Surya. 2021. "Performance and Emission Predictions of a CRDI Engine Powered with Diesel Fuel: A Combined Study of Injection Parameters Variation and Box-Behnken Response Surface Methodology Based Optimization." *Fuel* 290 (April), doi:10.1016/j.fuel.2020.120069.
- Ramalingam, Sathiyamoorthi, Sankaranarayanan Gomathinayakam, Venkattraman Mani, Jayaseelan Veerasundaram, and Sivakumar Kachapalayam. 2022. "Analysis of Optimising Injection Parameters and EGR for DICl Engine Performance Powered by Lemongrass Oil Using Box-Behnken (RSM) Modelling." *International Journal of Ambient Energy*, doi:10.1080/01430750.2021.2019111.
- Rostami, S., B. Ghobadian, and M. Kiani Deh Kiani. 2014. "Effect of the Injection Timing on the Performance of a Diesel Engine Using Diesel-Biodiesel Blends." *International Journal of Automotive and Mechanical Engineering* 10 (1): 1945–1958. doi:10.15282/ijame.10.2014.12.0163.
- Saiteja, Pajarla, and B. Ashok. 2022. "Study on Interactive Effects of CRDI Engine Operating Parameters Through RSM Based Multi-Objective Optimization Technique for Biofuel Application." *Energy* 255 (September): 124499. doi:10.1016/J.ENERGY.2022.124499.
- Saravanan, N., G. Nagarajan, K. M. Kalaiselvan, and C. Dhanasekaran. 2008. "An Experimental Investigation on Hydrogen as a Dual Fuel for Diesel Engine System with Exhaust Gas Recirculation Technique." *Renewable Energy* 33 (3): 422–427. doi:10.1016/J.RENENE.2007.03.015.
- Saravanan, S., G. Nagarajan, and S. Sampath. 2013. "Combined Effect of Injection Timing, EGR and Injection Pressure in NO<sub>x</sub> Control of a Stationary Diesel Engine Fuelled with Crude Rice Bran Oil Methyl Ester." *Fuel* 104 (February): 409–416. doi:10.1016/J.FUEL.2012.10.038.
- Sathiyamoorthi, R., and G. Sankaranarayanan. 2016. "Effect of Antioxidant Additives on the Performance and Emission Characteristics of a DICl Engine Using Neat Lemongrass Oil-Diesel Blend." *Fuel* 174 (June): 89–96. doi:10.1016/j.fuel.2016.01.076.
- Sathiyamoorthi, R., and G. Sankaranarayanan. 2017. "The Effects of Using Ethanol as Additive on the Combustion and Emissions of a Direct Injection Diesel Engine Fuelled with Neat Lemongrass Oil-Diesel Fuel Blend." *Renewable Energy* 101 (February): 747–756. doi:10.1016/j.renene.2016.09.044.
- Sathiyamoorthi, Ramalingam, Gomathinayakam Sankaranarayanan, Dinesh Babu Munuswamy, and Yuvarajan Devarajan. 2021a. "Experimental Study of Spray Analysis for Palmarosa Biodiesel-Diesel Blends in a Constant Volume Chamber." *Environmental Progress and Sustainable Energy* 40: 6. doi:10.1002/ep.13696.

- Sathiyamoorthi, R., G. Sankaranarayanan, and K. Pitchandi. 2017. "Combined Effect of Nanoemulsion and EGR on Combustion and Emission Characteristics of Neat Lemongrass Oil (LGO)-DEE-Diesel Blend Fuelled Diesel Engine." *Applied Thermal Engineering* 112 (February): 1421–1432. doi:10.1016/j.applthermaleng.2016.10.179.
- Sathiyamoorthi, Ramalingam, Gomathinayagam Sankaranarayanan, Mani Venkatraman, Dinesh Babu Munuswamy, and Rajendran Ravisankar. 2021b. "Environment-Friendly Fuel Cymbopogon Flexuosus: Analysis of Fuel Properties, Performance, and Emission Parameters of a Direct Injection Compression Ignition Research Engine." *Heat Transfer* 50 (7): 6589–6627. doi:10.1002/htj.22194.
- Senthil Kumar, J., and B. R. Ramesh Bapu. 2020. "Experimental Analysis of DI Diesel Engine Using Dual Biofuel Blended with Diesel." *International Journal of Ambient Energy* 41 (4): 431–434. doi:10.1080/01430750.2018.1472647.
- Senthil kumar, D., and S. Thirumalini. 2020. "Effect of Injection Parameters and EGR on Performance and Emissions in a CRDI Engine Fuelled with Cashew Nut Shell Biodiesel Blend." *International Journal of Ambient Energy* 43 (1): 1–37. doi:10.1080/01430750.2020.1796786.
- Senthil kumar, D., and S. Thirumalini. 2022. "Investigations on Effect of Split and Retarded Injection on the Performance Characteristics of Engines with Cashew Nut Shell Biodiesel Blends." *International Journal of Ambient Energy* 43 (1): 2251–2259. doi:10.1080/01430750.2020.1730961.
- Sharma, Abhishek, Yashvir Singh, Nishant Kumar Singh, Amneesh Singla, Hwai Chyuan Ong, and Wei Hsin Chen. 2020a. "Effective Utilization of Tobacco (Nicotiana Tabaccum) for Biodiesel Production and Its Application on Diesel Engine Using Response Surface Methodology Approach." *Fuel* 273: August. doi:10.1016/j.fuel.2020.117793.
- Sharma, Abhishek, Yashvir Singh, Avdhesh Tyagi, and Nishant Singh. 2020b. "Sustainability of the Polanga Biodiesel Blends During the Application to the Diesel Engine Performance and Emission Parameters—Taguchi and RSM Approach." *Journal of the Brazilian Society of Mechanical Sciences and Engineering* 42: 1. doi:10.1007/s40430-019-2102-3.
- Sindhu, R., G. Amba Prasad Rao, and K. Madhu Murthy. 2018. "Effective Reduction of NOx Emissions from Diesel Engine Using Split Injections." *Alexandria Engineering Journal* 57 (3): 1379–1392. doi:10.1016/J.AEJ.2017.06.009.
- Singh, Aparna, Shailendra Sinha, Akhilesh Kumar Choudhary, and H. Cheladurai. 2020a. "Biodiesel Production Using Heterogeneous Catalyst, Application of Taguchi Robust Design and Response Surface Methodology to Optimise Diesel Engine Performance Fuelled with Jatropa Biodiesel Blends." *International Journal of Ambient Energy* 43 (1): 1–12. doi:10.1080/01430750.2020.1789741.
- Singh, Aparna, Shailendra Sinha, Akhilesh Kumar Choudhary, Hitesh Panchal, Medhat Elkelay, and Kishor Kumar Sadasivuni. 2020b. "Optimization of Performance and Emission Characteristics of CI Engine Fueled with Jatropa Biodiesel Produced Using a Heterogeneous Catalyst (CaO)." *Fuel* 280 (July): 118611. doi:10.1016/j.fuel.2020.118611.
- Siva Prasad, K., S. Srinivasa Rao, and V. R. K. Raju. 2021. "Effect of Compression Ratio and Fuel Injection Pressure on the Characteristics of a CI Engine Operating with Butanol/Diesel Blends." *Alexandria Engineering Journal* 60 (1): 1183–1197. doi:10.1016/J.AEJ.2020.10.042.
- Sivaram, A. R., N. Prabhu, P. Ramanathan, R. Rajavel, and P. Prakash. 2020. "Investigation of Pongamia Pinnata with Nano Additives on Performance Characteristics of Diesel Engine." *TEST Engineering & Management* 83: 14332–14338.
- Suryawanshi, J. G., and N. V. Deshpande. 2005. "Effect of Injection Timing Retard on Emissions and Performance of a Pongamia Oil Methyl Ester Fuelled CI Engine." In *SAE Technical Papers*. SAE International. doi:10.4271/2005-01-3677.
- Teoh, Yew Heng, Heoy Geok How, Farooq Sher, Thanh Danh Le, Hwai Chyuan Ong, Huu Tho Nguyen, and Haseeb Yaqoob. 2021. "Optimization of Fuel Injection Parameters of Moringa Oleifera Biodiesel-Diesel Blend for Engine-out-Responses Improvements." *Symmetry* 13: 6. doi:10.3390/sym13060982.
- Wasiu, Saheed, Shaharin Sulaiman, Rashid Abdul Aziz, and Shaqil Azhar. 2018. "Effects of Different Injection Timings on the Performance and Emission Characteristics of the Direct-Injection Compressed Natural Gas Engine." *International Journal of Applied Engineering Research* 13 (1): 666–672. <http://www.ripublication.com>.
- Xiao, Helin, Xiaolong Yang, Ru Wang, Shengjun Li, Jie Ruan, and Hongling Ju. 2020. "The Effects Of Exhaust Gas Re-Circulation And Injection Timing On Combustion Performance And Emissions Of Biodiesel And Its Blends With 2-Methylfuran In A Diesel Engine." *Thermal Science* 24 (1 Part A): 215–229. doi:10.2298/TSCI190112304X.
- Yoon, Sam Ki, Jun Cong Ge, and Nag Jung Choi. 2019. "Influence of Fuel Injection Pressure on the Emissions Characteristics and Engine Performance in a CRDI Diesel Engine Fueled with Palm Biodiesel Blends." *Energies* 12 (20): 3837. doi:10.3390/en12203837.